



POWERSTEP

WP 3 – Biogas valorization and efficient energy management

***D 3.3: Full-scale technico-economical
performances of options for heat to
electricity conversion in WWTP***



The project "Full scale demonstration of energy positive sewage treatment plant concepts towards market penetration" (POWERSTEP) has received funding under the European Union HORIZON 2020 – Innovation Actions - Grant agreement^o 641661

Deliverable 3.3	<i>Full-scale technico-economical performances of options for heat to electricity conversion in WWTP</i>
Related Work Package:	WP3 Task 3
Deliverable lead:	Fraunhofer Institute for Physical Measurement Techniques IPM
Author(s):	Martin Kluge, David Bach, Patrick Ringwald
Contact for queries	Martin Kluge, David Bach
Grant Agreement Number:	n° 641661
Instrument:	Horizon 2020 Framework Programme
Start date of the project:	01.07.2015
Duration of the project:	36 months
Website:	www.powerstep.eu
Abstract	<p>The EU-funded project "POWERSTEP" aims on a full scale demonstration of energy positive sewage treatment plant concepts towards market penetration. In different case studies, innovative technologies for waste water treatment plants (WWTP) are developed, deployed and assessed. In the domain of heat-to-power technologies, the heat and power cogeneration plant (CHP) of a WWTP in Braunschweig, Germany was equipped with a thermoelectric generator (TEG) in order to boost the electrical efficiency of the CHP. This report summarizes the work that has been performed in TEG development and deployment at the case study site in Braunschweig; it performs a comparative analysis with an SRC/ORC unit and finally provides the technical and economical performances of options for full-scale heat electricity conversion in WWTP.</p>

Dissemination level of this document

<input checked="" type="checkbox"/>	PU	Public
<input type="checkbox"/>	PP	Restricted to other programme participants (including the Commission Services)
<input type="checkbox"/>	RE	Restricted to a group specified by the consortium (including the European Commission Services)
<input type="checkbox"/>	CO	Confidential, only for members of the consortium (including the European Commission Services)



Versioning and Contribution History

Version	Date	Modified by	Modification reasons
v.01	28-11-2017	Martin Kluge	Initial draft with table of content
v.02	22-01-2018	Martin Kluge, Patrick Ringwald, Dr. David Bach	First update with co-author inputs
v.03	12-02-2018	Martin Kluge, Dr. David Bach	Finalisation of chapters 4 and 5
v.04	16-02-2018	Martin Kluge, Dr. David Bach, Dr. Kilian Bartholomé, Dr. Olaf Schäfer-Welsen	External review version
v.05	16-03-2018	Martin Kluge, Dr. David Bach, Dr. Kilian Bartholomé, Dr. Olaf Schäfer-Welsen, Christoph Siemers, Christian Remy, Christian Loderer	Final version with corrections
v.06	28-03-2018	Martin Kluge	Final end version, reviewed by Christian Loderer



Table of Content

Dissemination level of this document	2
Versioning and Contribution History	3
Table of Content	4
List of figures.....	5
List of tables	7
Glossary	8
Executive summary.....	9
1. Introduction	10
1.1. Cogeneration of heat and power	10
1.2. Heat to power technologies overview	11
1.2.1. Rankine cycle	12
1.2.2. Thermoelectric conversion	12
1.3. Case study overview	13
2. Rankine cycle unit	16
3. Thermo-electrical generator for CHP	18
3.1. General aspects.....	18
3.2. Design of the TEG unit.....	19
3.2.1. Requirements analysis	19
3.2.2. Thermal/mechanical concept	21
3.2.3. Electrical concept	26
3.2.4. TEG integration in Braunschweig	28
3.3. Manufacturing and lab testing	32
3.3.1. Manufacturing	32
3.3.2. Lab testing of the TEG-unit stacks	33
3.4. Field deployment test.....	35
3.4.1. Installation of TEG in the exhaust system of the CHP	35
3.4.2. Results of field tests	36
3.4.3. Lessons learned from field testing	39
3.5. Projected full-scale performance of TEG.....	41
3.6. Projected TEG system price	46
4. Comparative analysis of H2P systems.....	50
4.1. System performance impact	50
4.2. Economic impact analysis	52
4.2.1. Direct comparison	52
4.2.2. Levelized cost analysis	58
4.3. Summary.....	59
5. Summary and Conclusion	60
6. Bibliography.....	61



List of figures

Figure 1: Schematic diagram of Rankine cycle [4].	12
Figure 2: Thermoelectric module design by Fraunhofer IPM	13
Figure 3: Waste water treatment plant (WWTP) in Braunschweig [11].	14
Figure 4: Four 16-cylinder gas engines (CHP units) installed in the CHP plant in Braunschweig.	14
Figure 5: HT SRC unit with 4-cylinder piston expander.	16
Figure 6: TEG integration in CHP (left: conventional CHP; right: CHP with TEG)	18
Figure 7: Exhaust gas heat exchanger of CHP	19
Figure 8: Simulations of the modular design concept; (Left: Single TEG-unit; Right: 3 TEG-units in serial configuration)	21
Figure 9: 3 Stage TEG concept for an 8kW Micro-CHP (Source: TE-BHKW project)	22
Figure 10: Schematic diagram of a heat exchanger [18]	22
Figure 11: Schematic diagram of a heat exchanger with thermoelectric layer (grey)	22
Figure 12: Thermal equivalent circuit of a thermos-electric generator.	23
Figure 13: Temperature dependent efficiencies of thermoelectric modules [10].	25
Figure 14: Equivalent circuit diagram of a thermoelectric generator [20].	26
Figure 15: Electrical output characteristics of thermoelectric devices in relation to constant temperature differences ΔT . (Grey: Voltage; Black: Power; Dotted: Progression of MPP) [21]	27
Figure 16: Thermoelectric generator prototype for Braunschweig case study	29
Figure 17: Interconnection model of employed TEM arrays.	29
Figure 18: Electrical concept for power generation and storage.	30
Figure 19: TEG Installation scheme	31
Figure 20: Schematic of measurement system with Raspberry Pi as central control unit.	32
Figure 21: Measurement system with Raspberry Pi B3 single board computer. Left: Front panel, Right: Internal wiring	32
Figure 22: Manufacturing of TEG. Left: TE-unit stacks before bundling the wire harness, Right: Mounting of TE-stacks on the rack.	33
Figure 23: Experimental setup hot air TEG test bench. (a) Sketch of the measurement setup. (b) Image of a TEG stack tested on the hot air test bench at Fraunhofer IPM.	34
Figure 24: Comparison of the power output of a TEG-unit and the differential pressure over the heat exchanger for stack B and C for a coolant inlet temperature of 20°C and a gas inlet temperature of about 450°C (hot air test bench at Fraunhofer IPM).	34
Figure 25: Comparison of the power output and differential pressure of the TEG-unit for stack A for a coolant inlet temperature T_c of 20 °C and 60 °C and a gas inlet temperature of about 450 °C up to 485 °C (hot air test bench at Fraunhofer IPM).	35
Figure 26: Simplified sketch showing the integration of the TEG in the exhaust system of the CHP. 1: By-pass valve, 2: standard heat exchanger, 3: rapid-action valve, 4: by-pass line for standard heat exchanger.	36
Figure 27: Overview of the TEG with electronic control unit/measurement electronics. 1: TEG; 2: electronic rack with MPPTs, electronic load, data acquisition unit; 3: coolant	



pump; 4: rapid-action exhaust gas valve; 5: main exhaust pipe of standard heat exchanger by-pass; arrows indicate the flow direction of the exhaust gas (photo taken 07.11.17).	36
Figure 28: Overview of the gas and coolant temperatures during field-test 2 (the indices mark the time of the taken measurements). M1: bypass-valve setting: 50 %, M2: bypass-valve setting: 25 %, M3: bypass-valve setting: 75 %.....	38
Figure 29: Maximum electrical power outputs of the TEG-units during field-test 2. (a) CAD image showing the location of the TEG-units in stacks A-C, (b) Comparison of measurements conducted with the usage of maximum power point trackers (MPPT). M1: by-pass valve set to 50 %, M2: 25 %, M3: 75 %. M2 lowest mass flow rate of exhaust gas, M3: highest mass flow rate. In total, depending on the operating conditions the TEG delivered an output power of about 400 to 530 $W_{el,TEG}$	39
Figure 30: TEG prototype after decommissioning	41
Figure 31: Heat exchange tubes inside the TEG with condensation and rust particles from upstream pipes.....	41
Figure 32: TEG systems for full scale performance calculation	42
Figure 33: Steps used to calculate the full-scale performance of a high performance TEG based on test bench measurement data (with $T_{GasIn}=450\text{ }^{\circ}\text{C}$).....	42
Figure 34: Performance comparison of a high performance and a low-cost TE-module on a module test bench ($T_{coolant}=75\text{ }^{\circ}\text{C}$). At $\Delta T=240\text{ K}$ the low cost module delivered ~10W and the high performance module ~12W which corresponds to a 20 % higher performance.....	43
Figure 35: Performance comparison of a high performance and a low-cost TE-module on a hot air test bench ($T_{coolant}=20\text{ }^{\circ}\text{C}$ and $60\text{ }^{\circ}\text{C}$). Overall, the mean increase in power for high performance vs. low-cost modules was about 19 %	44
Figure 36: BOM cost split of actual POWERSTEP prototype.....	47
Figure 37: BOM cost split of full scale TEG with high performance modules (prototype).	47
Figure 38: BOM cost split of full scale TEG with high performance modules in case of market penetration.....	48
Figure 39: Energy flow diagram of the MWM 50Hz PT 20128 KA in Braunschweig (based on datasheet [14])	50
Figure 40: Energy flow diagram of the MWM CHP with HT-SRC (according to preliminary manufacturer datasheet, without additional heat collect system)	51
Figure 41: Energy flow diagram of CHP with TEG (full-scale, two-stage TEG, based on bench test, without additional heat collect system)	51
Figure 42: ORC implementation scheme in AZV Südholstein	56
Figure 43: LCOE for various renewable energy sources [31]	59

List of tables

Table 1: Target performance of HT-SCR system	16
Table 2: Technical parameters of HT-SCR system.....	17
Table 3: Thermoelectric generator thermal requirements	20
Table 4 Exhaust gas analysis of CHP module 1 [15]	20
Table 5 Optimum temperature distribute in a CHP TE conversion unit in matched condition	24
Table 6 Risk analysis and mitigation (operation phase)	30
Table 7: Summary of hot air test bench measurements for TEG stacks A-C.	35
Table 8: Overview of the conducted field tests	37
Table 9 Detailed results of field test 2.(Note: Module A1 delivering 50% of typical power)39	
Table 10: Performance result of simulated two stage design.	44
Table 11: Projected performances of the TEG configurations for exhaust gas mass flow rate of about 3 944 kg/h and an inlet gas temperature of 450 °C.....	45
Table 12: Summary of impact of heat-2-power system on the overall performance of the CHP. 52	
Table 13: Electricity price components [27].....	53
Table 14: ROI and simple payback period calculation of TEG in Braunschweig.	55
Table 15: ROI and simple payback period calculation of ORC in AZV Südholstein.	57



Glossary

CHP	Combined heat and power
EUR	Euro
H2P	Heat-to-Power
HT-SRC	High Temperature Steam Rankine Cycle
kW	kilo-watt
kW_{el}	kilo-watt electricity
kW_{th}	kilo-watt thermal
kWh	kilo-watt hour
LCOE	Levelized Cost of Electricity
l	litre
MWh	Mega-watt hour
ORC	Organic Rankine Cycle
PE	Person Equivalent
PP	Payback Period
ROI	Return on Invest
SRC	Steam Rankine Cycle
TEG	Thermo-electric generator
TEM	Thermo-electric module
WWTP	Waste water treatment plant



Executive summary

The EU-funded project "POWERSTEP" aims on a full scale demonstration of energy positive sewage treatment plant concepts towards market penetration. In different case studies, innovative technologies for waste water treatment plants (WWTP) are developed, deployed and assessed.

This report introduces different heat-to-power technologies; it described in detail the design and manufacturing and field deployment of a TEG for the CHP installation in Braunschweig and it concludes with a comparative technico-economical analysis of the two technologies of thermoelectric conversion and Rankine cycle (ORC/SRC).

The construction and design of the thermoelectric generator has been closely aligned with the CHP system of the case study site in Braunschweig. One of the main important topics was the selection of the right thermoelectric material for the application temperature range: High performance Bi_2Te_3 was chosen to be the best solution for exhaust gas temperatures of 450°C - 180°C and coolant temperatures of 60 - 80°C . For the pilot integration, several possible positions on the exhaust line have been studied and measurement electronics along with a safety concept have been developed and deployed. The final implementation and field tests lead to important insights on practical issues, like the operation in harsh industrial environment and more. The lessons learned give an important input for the future development of TEG.

The comparative technico-economical analysis based on the Braunschweig scenario showed, that the TE-technology allows raising the CHP electrical yield by +1.5 %. Assuming a future specific investment cost of 4 000 EUR/kW_{el}, it is expected to amortize in approximately 5.3 years. As today some prototype part costs are still more than 10 times higher than targeted, the authors expect that a significant impact is needed from high volume markets in order to reach into the target cost ranges for this application class. The supply chain for the technology is still under development and the main building blocks are heat exchangers, thermoelectric modules and power electronics.

In direct comparison with SRC/ORC technology, potential main benefits of thermoelectrics are low investment costs as well as the low operation and maintenance cost. The levelized cost of electricity production from the TEG could be around 15 ct/kWh (with a utilization of 4 207 h/a).

For the studied CHP size of 710 kW_{el}, using SRC potentially outperforms the TEG by a factor of 4-5 in electricity production. The electrical yield improvement could reach up to +6 % for SRC or even +8 % in case of usage of an ORC. Despite the fact, that both investment costs and maintenance costs are higher than for TEG, new ORC technology could allow reaching a levelized cost of electricity of 5.5 to 8.9 ct/kWh. However, existing ORC implementations like in WWTP Hetlingen can also range at higher values with 20 ct/kWh (with a utilization of 2 500 h/a).

It can be concluded that a future TEG would be based in a competitive cost range among electricity production from Biogas technology; however, as explained above the latest ORC technology could be potentially cheaper and more effective in this application class. The results may give a first indication that TEG is a technology that is favourable for smaller CHPs.



1. Introduction

The implementation of safe and efficient wastewater treatment systems is essential to satisfy the global water demand, safeguard the environment, protect public health and meet sustainability goals. Energy-positive wastewater treatment plants (WWTPs) create an enabling environment for greener, smarter and more circular cities.

The EU-funded project "POWERSTEP" [1] aims on a full scale demonstration of energy positive sewage treatment plant concepts towards market penetration. In different case studies, innovative technologies for WWTP are developed, deployed and assessed.

In the domain of heat-to-power (H2P) technologies, the heat and power cogeneration plant (CHP) of a WWTP in Braunschweig, Germany was equipped with a thermoelectric generator (TEG) in order to boost the electrical efficiency of the CHP. The motivation was to make use of excess heat at WWTP, which frequently have net surplus heat from CHP operation. The goal was to demonstrate the new technology of TEG at a WWTP-CHP (design, operation, performance) and to meet the challenge of choosing the correct design for the available temperature levels. In parallel the performance data of a comparable Rankine cycle unit was investigated as an alternative means to generate electricity from heat and to compare economic feasibility/payback between the H2P approaches.

This report summarizes the work that has been performed in TEG development and deployment at the case study site in Braunschweig, it performs a comparative analysis with an SRC/ORC unit and finally provides the technical and economical performances of options for full-scale heat electricity conversion in WWTP.

1.1. Cogeneration of heat and power

The method of cogeneration of heat and power (CHP) is a key solution to improve energy efficiency and thus to reduce CO₂ emissions. This following introduction was originally published in [2] and [3].

A CHP plant consists of an electrical generator combined with equipment for recovering and using the heat produced by that generator. The generator can be a prime mover such as a gas turbine or a reciprocating engine. Alternatively, it may consist of a steam turbine generating power from high-pressure steam produced in a boiler.

Gas-engine CHP packages are available in a range of electrical outputs – from less than 50 kW_{el} to around 1 000 kW_{el}. The electrical generating efficiency of these packages is typically around 30 %, and units can be operated at reduced load with very little drop in engine efficiency. The ratio of recovered heat to electricity generated in a gas-engine package is typically around 1.5:1.

The gas engines used in CHP packages are internal combustion engines that operate on the same familiar principles as the engines in vehicles: they use spark plugs to ignite the fuel in the engine and are sometimes referred to as 'spark-ignition engines'. These engines have been designed for operation on a gaseous fuel, most commonly natural gas. Many engines can operate on supply pressures as low as 0.1 bar gauge (barg), the pressure at which gas is usually available from the gas supply system. In situations where



the gas pressure is inadequate, a small pressure booster unit can be installed as part of the CHP package.

Since the CHP engine drives an electrical alternator, the engine must be designed to operate at constant speed and at exactly the same frequency as the mains supply, even though the fuel input and electrical output of the CHP package may be variable. The gas engines used in CHP packages typically operate at 1 500 rpm: units above 1.3 MW_{el} may operate at 1 000 rpm.

Engines and their lubricating oil must be cooled to prevent overheating. This cooling system provides heat in the form of hot water, which is produced whenever the engine is running, irrespective of whether or not it can be used. In a packaged CHP unit, the engine/lubricating oil cooling system is usually connected to a heat exchanger that also recovers heat from the engine exhaust gases. This helps to maximise the combined thermal and electrical efficiency of the engine. Cooling system heat and exhaust heat are recovered in roughly equal proportions from a gas engine CHP package. The heat from the engine is typically recovered at around 80 °C, but some engines can operate using pressurised hot water, which delivers heat at up to 120 °C. The exhaust gas, which is used as an additional heat source, may vary in a wide temperatures range from 450-650°C, depending on the engine type and fuel.

If the recovered heat is not all required by the site, the surplus must be dissipated using a cooling system. Alternatively, the power output must be modulated to match the heat demand. The cooling system is similar in principle to a vehicle engine's radiator and needs to be of sufficient capacity to maintain the flow of water to the engine at the correct temperature. All engines are equipped with automatic controls, which shut down the engine if it starts to overheat.

Gas engines vibrate, and the package design usually incorporates supports to dampen the effect of any vibrations on the floor beneath the package and on pipework. The noise levels from gas engines can also be a nuisance, particularly if the noise resonates within a building, and nearly all CHP packages are designed to act as effective acoustic enclosures to limit this problem. The enclosure itself is ventilated to avoid overheating.

All engines have moving parts, some of which suffer gradual wear and, therefore, require maintenance or replacement at regular intervals. Some of the routine maintenance tasks may be carried out while the engine is operating, but regular shutdowns for maintenance and servicing are also required. The total downtime is not excessive and high levels of engine availability can be achieved (typically 90 %).

1.2. Heat to power technologies overview

The term heat to power technologies (H2P) summarizes the technologies that can be used to convert heat into other kinds of power, e.g. into mechanical or electrical power.

In the context of a CHP with internal combustion engine the most widespread source of heat being utilized for H2P is the exhaust heat of the engine. Although the engines in power generation which are already very efficient they still have a significant waste



heat power flow that can be exploited to achieve an even higher electrical and/or mechanical output. The following two technologies are discussed in this document.

1.2.1. Rankine cycle

The most wide spread technology for H2P is the Rankine cycle. It can be considered as a heat engine with a vapour power cycle. The common working fluid is water (SRC) or organic fluids (ORC). Power can be extracted either electrically, using a generator set, or mechanically, by directly applying the rotation of the turbine. The vapour power cycle consists out of four main steps as shown in Figure 1.

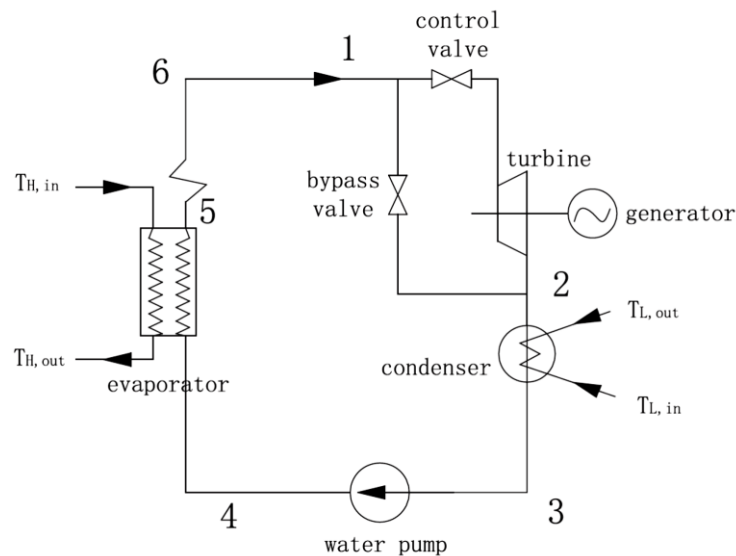


Figure 1: Schematic diagram of Rankine cycle [4].

They can be explained as follows:

Step 1 to 2: Isentropic expansion inside a steam turbine - An isentropic process, in which the entropy of working fluid remains constant. Steam expansion causes movement of the turbine and thus allows extracting mechanical energy.

Step 2 to 3: Isobaric heat rejection in a condenser unit - An isobaric process, in which the pressure of working fluid remains constant.

3 to 4: Isentropic compression by a pump - During the isentropic compression process, external work is done on the working fluid by means of pumping operation.

4 to 1: Isobaric heat supply using a steam generator or boiler - During this process, the heat from the high temperature source (=CHP exhaust) is added to the working fluid to convert it into superheated steam.

1.2.2. Thermoelectric conversion

Another technology for H2P is the thermoelectric conversion. The thermoelectric effect was discovered in 1821 by Thomas Johann Seebeck. He observed that a temperature difference between two dissimilar electrical conductors or semiconductors produces a voltage difference between the two substances. Ever since the ratio between the gen-



erated voltage and the causing temperature difference is called the Seebeck-coefficient.

Modern society uses thermoelectrics mostly for electrical cooling applications like small, portable refrigerators, cooling boxes, or chip coolers in telecommunications. In deep space applications so called radioisotope thermoelectric generators (RTGs) have been successfully deployed to convert heat from radioactive decay into electricity in order to power satellites during their mission [5].

In more recent times, the automotive industry has discovered that the technology of converting heat-to-power by thermoelectrical conversion could allow to save fuel and to reduce the CO₂ emissions of modern passenger cars or trucks. Today, large R&D efforts aim on developing the right materials and robust, cost-efficient designs to establish thermoelectric generators as automotive standard components [6], [7], [8], [9], [10]. The main technological benefits are compactness, low weight, scalability and a maintenance-free operation.

Thermoelectrics are typically applied in the form of modules (TE-modules). They consist out of n- and p-type TE materials (legs) which are connected thermally in parallel and electrically in series. The waste heat is converted by creating a heat flow through the TE module (Figure 2) which generates an electrical current. The electrical connection between the TE legs is realized by brazing or soldering the legs onto a ceramic carrier substrate with metallic conductor pads. The numbers and dimensions of the TE legs differ according to the intended application of the module. The correct TE-material choice is strongly depending on the operation temperatures of the modules (see chapter 3.2.2.3).

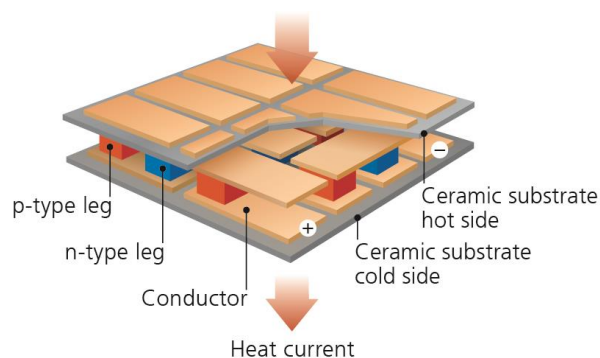


Figure 2: Thermoelectric module design by Fraunhofer IPM

1.3. Case study overview

The WWTP in Braunschweig (Figure 3) was built in 1979 and upgraded several times (1986, 1991, 2001). It is located in the suburb Braunschweig Steinhof, in the north of the city and is connected to approx. 140 000 households, treating 350 000 PE or 22 billion cubic meters of waste water per year [11]. This number includes the leachate water from the nearby landfill site in Watenbüttel.





Figure 3: Waste water treatment plant (WWTP) in Braunschweig [11].

From the mechanical and biological treatment of sewage and leachate water, the WWTP produces large amounts of sludge which is converted to biogas in anaerobic digestion and then co-fired in a CHP together with landfill gas from Watenbüttel and biogas from an attached composting facility.

The heat and electrical energy produced by the CHP plant are either consumed directly on site, or sold/fed into the available grid. Please see the POWERSTEP deliverable 3.4 "Recommendations for improved energy management at waste water treatment plants" for details on optimal usage strategies.

The Braunschweig cogeneration plant was built in 1991 and last modernized 2009. It includes four 16-cylinder gas engines / CHP units (Figure 4) that can be selectively operated in order to ensure maximum flexibility. In sum the theoretical total capacity is 2.84 MWh_{el} and 2.72 MWh_{th} (when utilising exhaust gas heat exchangers). To reach an optimal combustion, the methane content of the gas is adjusted by mixing biogas and landfill gas. The target methane content is min. 50 % (lean burn). Today the plant operation is mostly based on the electricity demand.



Figure 4: Four 16-cylinder gas engines (CHP units) installed in the CHP plant in Braunschweig.

Today, according to the manufacturer MWM, the efficiency reached by one CHP unit is approximately 41.5 % in electricity production and 39.7 % in the production of useful heat. The useful heat can be split into 355 kW_{th} from engine cooling and 330 kW_{th} from exhaust gas heat, which is generated by cooling the gas from 450 °C to 180 °C with an exhaust gas heat exchanger. The heat to power ratio (H/P) of the unit is 0.957 which represents a high electrical efficiency in compare to the state-of-art CHPs. By integrating novel heat to power technologies like SRC, ORC or TEG into the exhaust line of the CHP unit, this ratio can be further improved, thus resulting into a longer, electrically more efficient, operation when supplying a given heat demand.



2. Rankine cycle unit

The Rankine cycle unit that had been installed in Braunschweig was developed by the company CONPOWER Technik Projekt GmbH & Co. KG in Kaufungen. The operation is based on a high temperature steam Rankine cycle (HT-SRC) using a 4-cylinder piston expander (Figure 5). The major benefit of using water as a medium for producing superheated steam is that it can be directly evaporated without intermediate thermo-oil circuit using evaporation temperatures of up-to 500 °C [12]. This allows raising the overall efficiency. In the installation, the direct-evaporator is placed instead of conventional exhaust gas heat exchanger of one CHP unit (see chapter 3.2.1 for technical data).



Figure 5: HT SRC unit with 4-cylinder piston expander.

The unit in Braunschweig was designed to work in combination with the MWM TCG 2016C V16 engine installed in the CHP. The target performance data of the HT-SCR is given in Table 1. The underlying technical parameters are given in Table 2.

Table 1: Target performance of HT-SCR system

Heat input	~282 kW _{th} (+80 kW _{th} heat collect system)
Heat output	~305 kW _{th}
Electricity production	~43 kW _{el}
Conversion efficiency (electricity/heat input)	~15 %

Unfortunately the supplier had to file for bankruptcy before the system was put in operation. In chapter 4 the target performance will be compared against other heat-to-power systems.

Table 2: Technical parameters of HT-SCR system

Input exhaust gas temperature	~ 450 °C
Output exhaust gas temperature (target)	~ 180 °C
Mass flow exhaust gas side	~ 3,746 kg/h
Backpressure exhaust gas side (max.)	20 mbar
Exhaust gas medium	Exhaust gas from natural gas firing
Input coolant temperature	45 - 65 °C
Output coolant temperature (target)	85 °C
Volume flow coolant side	11.1 m ³ /h
Backpressure coolant side (max.)	100 mbar
Coolant medium	Water (H ₂ O)



3. Thermo-electrical generator for CHP

Beginning with a general introduction to thermoelectric generators for CHP this chapter explains the design of the TEG unit applied in Braunschweig.

3.1. General aspects

The application of thermoelectric generators to cogeneration plants using reciprocating engines is a logical supplement to the recent developments of the automotive industry. Whilst a passenger car or truck presents a very harsh operational environment with very dynamic temperature changes, extreme absolute temperatures, strong vibrations, shocks and corrosive media, the stationary application of a TEG in a CHP seems to be much less demanding. However, the major difference to the automotive industry is the operation time. For a CHP application, this could be as much as 8 500 hrs per year.

In case of CHP based on reciprocating engines, the thermo-electric generators (TEG) are installed into the exhaust line replacing the existing exhaust gas heat exchangers (see chapter 1.1).

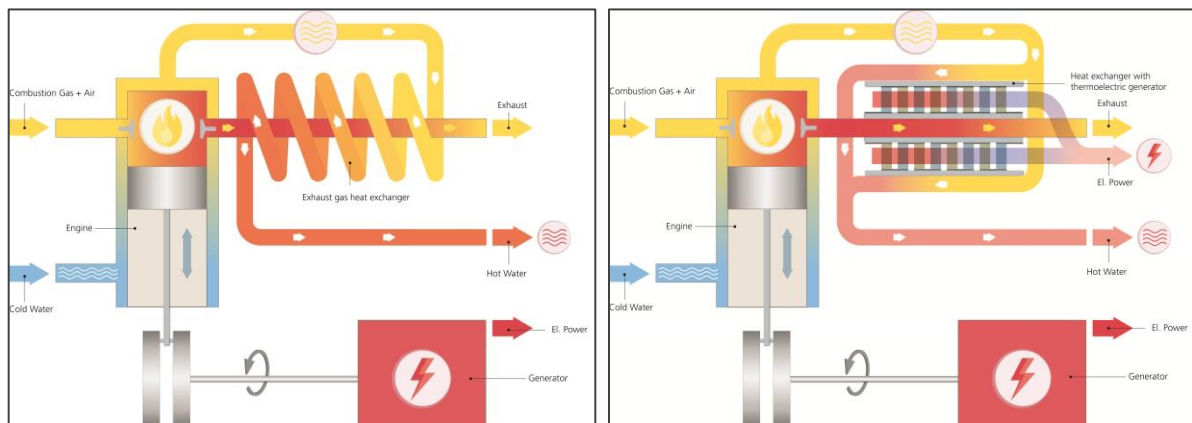


Figure 6: TEG integration in CHP (left: conventional CHP; right: CHP with TEG)

The reciprocating engines of biogas fed CHP are constructed very similar to industrial gasoline engines. They are widely spread for the use in biogas plants, as the technology is very well established and robust. Their operating time can reach up to 8 500 hrs per year. The overall energy efficiency is typically around 80 % [3], proving the systems to be very efficient against their competition (e.g. stirling engines, gas turbines).

The main drawback of the technology is the required maintenance: Every 2 500 to 4 000 hrs a servicing of the engine has to take place in order to change engine oil, filters, sparking plugs, pistons etc. [13].

With regard to the heat exchangers installed in the exhaust line, sooting and the deposition of oil and sulfurous residuals require a cleaning interval of approximately every 10 000 hrs. Continuous operation without servicing will lead to a loss in overall efficiency, increased backpressure and in worst case, engine failure.

3.2. Design of the TEG unit

3.2.1. Requirements analysis

Prior to the design of the TEG unit, the existing situation in Braunschweig was analysed. The CHP plant in Braunschweig Steinhof was installed in 2005 by the Mannheim based company MWM. MWM develops products, services, and technologies for decentralized energy supply with gas engines. The technical data of the installation called "50Hz PT 20128 KA Braunschweig" is listed in [14].

The basic requirements of the resulting full scale TEG system to be installed on one engine exhaust can be derived directly from the existing heat exchanger. With a size of $3.65 \times 0.51 \times 0.85 \text{ m}^3$ and a dry weight of 510 kg, the nominal thermal power provided by the APROVIS heat exchanger is $331 \text{ kW}_{\text{th}}$, resulting from a temperature decrement of exhaust gas from $450 \text{ }^\circ\text{C}$ to $180 \text{ }^\circ\text{C}$ at an exhaust gas mass flow rate of $3\,944 \text{ kg/h}$. Calculated from these values the thermal efficiency of one unit is approximately 73 %. The maximum allowed backpressure on the exhaust side is 11 mbar. On the coolant side the input temperature is $80 \text{ }^\circ\text{C}$. The coolant medium is water. Figure 7 shows the heat exchanger installed in Braunschweig Steinhof.



Figure 7: Exhaust gas heat exchanger of CHP

As the full-scale TEG is intended to fully replace this exhaust gas heat exchanger, the thermal requirements can be concluded to be as follows:



Table 3: Thermoelectric generator thermal requirements

Input exhaust gas temperature	450 °C
Output exhaust gas temperature (target)	180 °C
Mass flow exhaust gas side	3 944 kg/h
Backpressure exhaust gas side (max.)	11 mbar
Exhaust gas medium	Combustion gas (CO ₂ , H ₂ O, N ₂ , ...)
Input coolant temperature	80 °C
Output coolant temperature (target)	90 °C
Volume flow coolant side	29.4 m ³ /h
Backpressure coolant side (max.)	80 mbar
Coolant medium	Water (H ₂ O)

The exhaust gas composition is monitored on an annual basis by DEKRA. The following table shows the results for the year 2015.

Table 4 Exhaust gas analysis of CHP module 1 [15]

Parameter	Mean concentration	Maximum concentration	Concentration Limit	Mean mass flow	Max mass flow	Mass flow limit
	[g/m ³]	[g/m ³]	[g/m ³]	[kg/h]	[kg/h]	[kg/h]
NO _x as NO ₂	0.45	0.48	0.5	1.012	1.068	-
CO	0.025	0.025	0.65	0.057	0.057	-
SO _x as SO ₂	0.002	0.004	0.31	<0.005	0.009	-
Formaldehyd	0.010	0.011	0.06	0.023	0.025	-
	[mg/m ³]	[mg/m ³]	[mg/m ³]	[g/h]	[g/h]	[g/h]
Cancerous substances ¹	< 0.3	< 0.3	1	0.31	<0.31	-
HF	0.6	0.7	-	1.3	1.5	15
HCL	1.3	2.1	-	2.9	4.8	150

Benzol, Vinylchlorid, 1,2 Dichlorethan, Trichlorethan

3.2.2. Thermal/mechanical concept

3.2.2.1 Modular design approach

To ensure scalability and design flexibility, the Fraunhofer IPM concept for building a TEG for CHP applications follows a modular design approach. Initially developed in the TEWAB-Project funded by Badenova Innovationfonds [16], this modular approach has been carried over to other CHP projects.

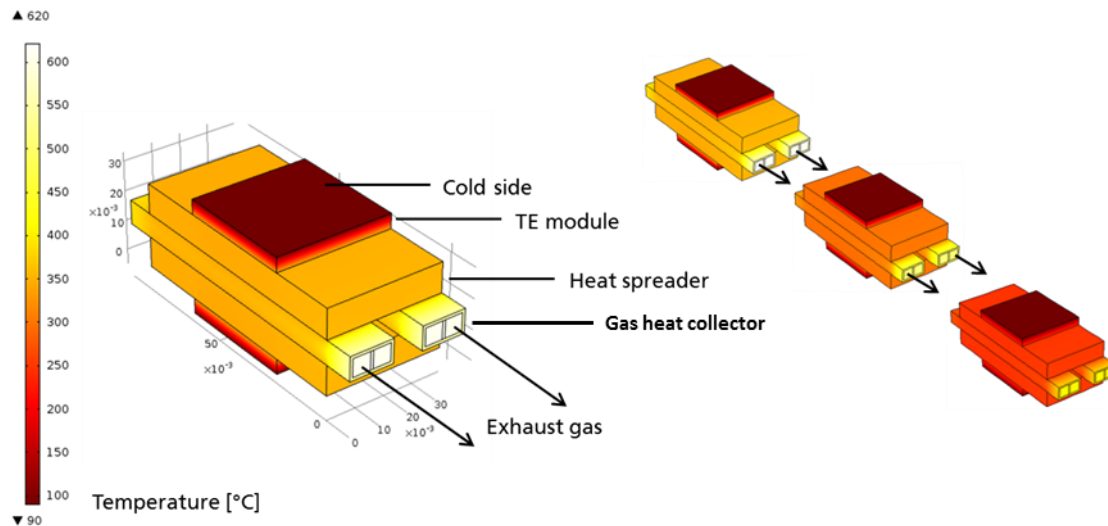


Figure 8: Simulations of the modular design concept; (Left: Single TEG-unit; Right: 3 TEG-units in serial configuration)

A single TEG-unit consists out of an exhaust gas heat collector, a heat spreader, TE module(s) and the cold side (Figure 8). Typically it also includes a cooler that is not shown in this figure. The TEG units can be operated either in parallel or in a serial configuration. The later configuration allows individual matching of the thermoelectric material and temperatures for each stage of the TEG as the gas temperature naturally drops in the flow direction when heat is extracted.

As a first result of the TE-BHKW project [17] arrays of four TE-modules will be integrated on the heat collector device. The heat spreader function is directly integrated into the heat collectors by using thermally highly conductive materials like copper. For the EU-funded TE-BHKW project, the heat collector geometry was analysed, optimised by CFD analysis and later validated by bench tests.



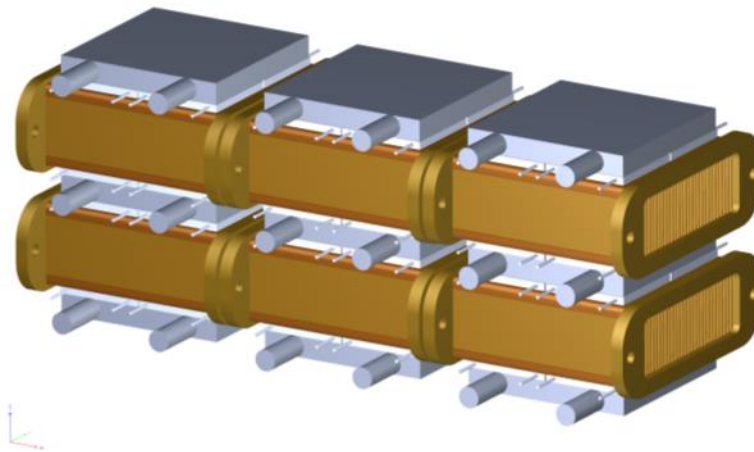


Figure 9: 3 Stage TEG concept for an 8kW Micro-CHP (Source: TE-BHKW project)

The optimised heat collector geometry was also implemented in the Powerstep project and will be explained in the following chapters.

3.2.2.2 Heat transfer

The process of heat transfer inside a thermoelectric generator unit is significantly different from a classical heat exchanger. As the heat has to pass through the semiconducting material of the thermoelectric conversion layer, the heat transfer capability of a TEG is in general lower in compare to a classical heat exchange device.

The VDI Heat Atlas [18] describes the schematic diagram of a heat exchanger and its main parameters as shown in Figure 10.

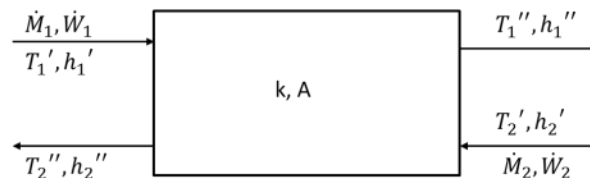


Figure 10: Schematic diagram of a heat exchanger [18]

Its input and output parameters are the mass flow rates \dot{M}_1 , \dot{M}_2 , the heat capacities rates \dot{W}_1 , \dot{W}_2 , the specific enthalpies h_1 , h_2 and the temperatures T_1 , T_2 . The heat transfer coefficient k and the surface area A are variables to quantify the heat exchange.

When introducing a thermoelectric conversion layer into a heat exchanger, the classical approach needs to be altered, considering the coupling effects between the thermal and electrical domain.

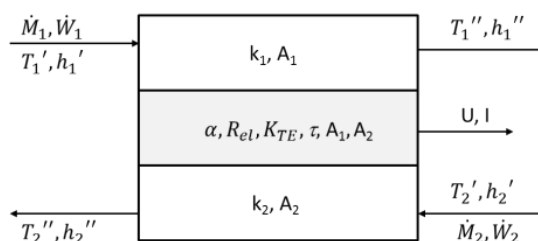


Figure 11: Schematic diagram of a heat exchanger with thermoelectric layer (grey)



Figure 11 shows a modified diagram introducing a thermoelectric layer characterised by the Seebeck coefficient α , the electrical resistance R_{el} , the thermal resistance K_{TE} and the Thomson coefficient τ , as well as the input and output contact areas A_1 , A_2 . In case of a thermoelectric generator, the heat transfer across these contact areas is strongly depending in the thermoelectric layer and the imposed current I or voltage U .

In his doctoral dissertation Michael Freunek explains the fundamentals of thermal and electrical matching of a thermo-electric generator device under consideration of the Joule, Peltier and Thompson effects [19]. He suggests using a simplified thermal equivalent circuit shown in Figure 12. Here the white rectangles represent thermal resistances; K_h stands for the source (e.g. an exhaust gas heat collector), K_{TE} for the thermo-electric module layer and K_c for the sink (e.g. a liquid cooler). T_h and T_c represent the hot-side and cold-side temperatures of the TE-material.

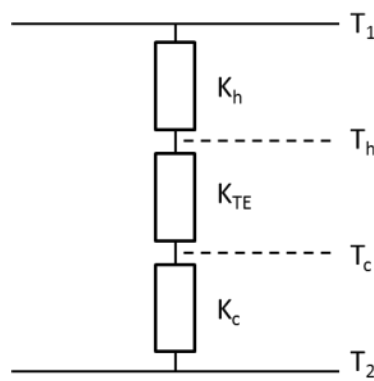


Figure 12: Thermal equivalent circuit of a thermos-electric generator

Combining both approaches, the heat flux equations for the heat exchange can be written as follows:

$$\text{Equation 1} \quad \dot{Q}_{in} = \frac{1}{K_h} \cdot (T_1 - T_h) = \dot{W}_1 \cdot (\vartheta_1' - \vartheta_1'');$$

$$\text{Equation 2} \quad \dot{Q}_{out} = \frac{1}{K_c} \cdot (T_c - T_2) = \dot{W}_2 \cdot (\vartheta_2'' - \vartheta_2');$$

The thermal resistances of the finite source K_h (e.g. an exhaust gas heat collector) and finite sink K_c (e.g. a liquid cooler) can be expressed using the heat transfer coefficient k and the surface area A of the model in Figure 11: Schematic diagram of a heat exchanger with thermoelectric layer.

$$\text{Equation 3} \quad K_h = \frac{A_1}{k_1};$$

$$\text{Equation 4} \quad K_c = \frac{A_2}{k_2};$$

Due to the law of conservation of energy, in a system without loses Equation 1 and Equation 2 can also be used to calculate the electrical power output of the TEG P_{el} .

$$\text{Equation 5} \quad P_{el} = \dot{Q}_{in} - \dot{Q}_{out};$$

The thermoelectric generator electrical and thermal efficiencies are defined by Equation 6 and Equation 7.

$$\text{Equation 6} \quad \eta_{el} = \frac{P_{el}}{\dot{Q}_{in}};$$



Equation 7 $\eta_{th} = \frac{\dot{Q}_{out}}{\dot{Q}_{in}};$

Following the analytical approach to maximise the electrical power of a TEG as described in [19], the result is that for a given thermal resistance of source and sink, the optimum thermal resistance of the TE-layer $K_{TE,opt}$ should be calculated by Equation 8. This equation is assuming operating in an electrical matched load condition; this means the electrical load current (the corresponding load resistance) is adjusted in order to obtain a maximum electrical output power condition.

Equation 8 $K_{TE,opt} = (K_C + K_H)\sqrt{1 + ZT_C};$ or $\frac{K_{TE,opt}}{(K_C + K_H)} = \sqrt{1 + ZT_C};$

In this equation the expression ZT_0 is relating to the material specific thermoelectric figure of merit Z , multiplied with the cold side temperature of the system T_C in Kelvin. The theoretical calculation assumes ZT_C to be constant².

In the described condition about 50% of the available temperature difference should occur on the thermoelectric layer [19]. The remaining 50% are distributed across the source and the sink. This finding allows predicting the temperature distribution, selecting the appropriate material and approximating the electrical power output of the system.

Application to CHP use case scenario

As the heat transfer coefficient of forced convection in liquids is typically 2-80 higher than the heat transfer coefficient of forced convection in gases [18], the following optimum temperature distribution can be assumed for the TE conversion unit in a CHP application (Table 5).

Table 5 Optimum temperature distribute in a CHP TE conversion unit in matched condition

Device section	Temperature distribution (Total 100%)
Heat collector (ex. gas)	33 % - 49 % of 100 % ΔT
Thermoelectric layer	~ 50 % of 100 % ΔT (matched load condition)
Cooler (liquid)	0.6 % - 17 % of 100 % ΔT

As a direct consequence of the intrinsically low temperature difference across the heat collector, the maximum input heat flux and therefore also the heat exchange capability of a TE-conversion unit is limited to < 50 % of the available exergy of the exhaust gas, when at the same time maximising the electrical power output.

If a higher heat exchange rate is desired in combination with maximum electrical power output, it is possible to add a consecutive heat exchange state, extracting the remaining exhaust gas exergy into the available cooling circuit.

² For of the shelf Bi_2Te_3 components that are operating from room temperature, a typical value of ZT_C is 0.8 [18].



3.2.2.3 Thermoelectric conversion layer

In recent years numerous TE materials have been developed, integrated into TE modules and tested in applications. They are used to form the thermoelectric conversion layer that has to follow the principles explained in chapter 2.2.2.2 and fulfil the requirements listed in 2.2.1.

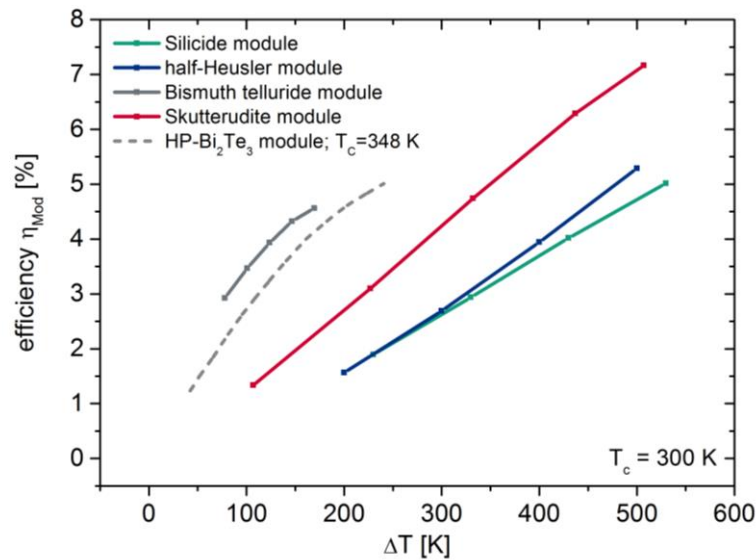


Figure 13: Temperature dependent efficiencies of thermoelectric modules [10].

The solid lines in Figure 13 represent typical efficiencies of TE-modules measured for various hot side temperature differences against room temperature [10]. High temperature materials like silicide and half-Heusler alloys exhibit their highest efficiencies at hot side temperatures of around 550 °C. The medium application temperature range is covered by the highly efficient but yet unstable Skutterudites and the lower range by Bismuth telluride with usage temperatures of typically up to 200 °C. In addition, new high performance (HP) Bi₂Te₃ modules have recently been developed that allow for a higher operation at temperatures of up to 315 °C (dashed line, Figure 13).

The selection of the most suitable TE-material has to be based on the expected operation temperatures. In case of the CHP application these operation temperatures can be approximated from the requirement data provided in Table 3. By applying equations 9, 10 the average gas temperature T_1 results in 304.5 °C, the average coolant temperature T_2 in 87.5 °C. Finally, respecting the design principle of thermal matching, the temperature difference across the TE-Material can be concluded to be approximately 125 K by using Equation 11 and the data of Table 5.

$$\text{Equation 9} \quad T_1 = \frac{(T_1' - T_1'')}{\ln(T_1') - \ln(T_1'')}$$

$$\text{Equation 10} \quad T_2 = \frac{(T_2'' - T_2')}{\ln(T_2'') - \ln(T_2')}$$



$$\text{Equation 11 } \Delta T_{TE} = (T_1 - T_2) \cdot 0.5$$

From Figure 13 it can be concluded that the most suitable thermoelectric material for the use case is Bi_2Te_3 . Its expected electrical conversion efficiency is approximately 3.0 – 3.5 %.

3.2.3. Electrical concept

TE-converter interface

From the electrical point of view, a single TE-module can be approximated with a DC voltage source in series with an internal resistance (Figure 15).

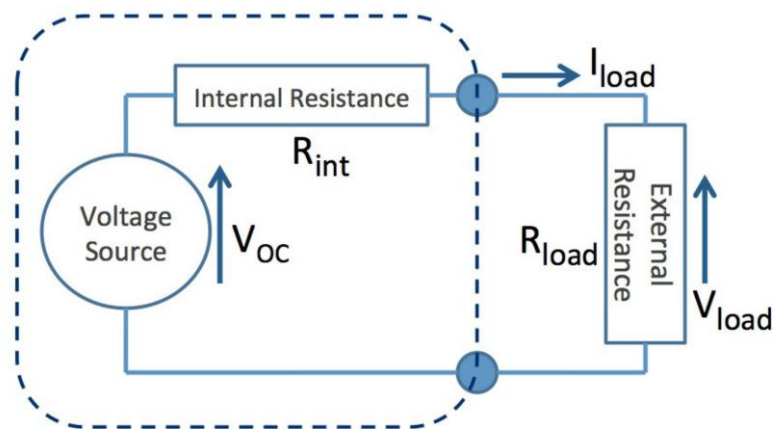


Figure 14: Equivalent circuit diagram of a thermoelectric generator [20]

The open-circuit voltage V_{OC} , the internal resistance R_{int} and therefore the short-circuit current I_S are considered to be constant for a constant/steady state temperature difference ΔT across the TEG device. At any given ΔT the load power is parabolic (Figure 15) and has only one maximum power point (MPP) which occurs when $R_{int} = R_{load}$. The voltage V_{load} and in turn the load power P_{tem} are dependent on the load resistance.

$$\text{Equation 12 } V_{load} = V_{OC} - R_{int}I_{load}$$

The load current I_{MP} and voltage V_{OC} at the MPP are given by Equation 13 and Equation 14.

$$\text{Equation 13 } I_{MP} = \frac{V_{OC}}{2R_{int}}$$

$$\text{Equation 14 } V_{MP} = \frac{V_{OC}}{2}$$

The maximum power that can be generated by the TEG can be written as

$$\text{Equation 15 } P_{max} = \frac{V_{OC}^2}{4R_{int}}$$

If the load resistance is smaller than R_{int} , the current I_{load} increases hence the Joule heating and the Peltier effect inside the TE-module increase leading to a decrease of ΔT across the module. In summary the right hand side of the MPP results in higher thermal transport and consequently to decreased efficiency, whereas the left side exhibits a lower thermal transport and increased efficiency.

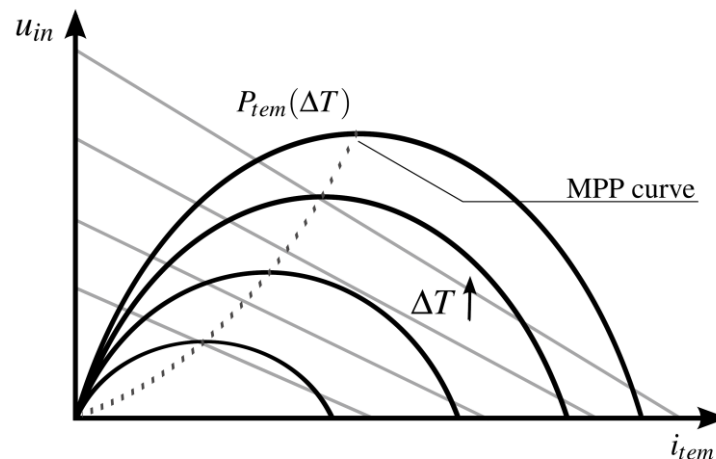


Figure 15: Electrical output characteristics of thermoelectric devices in relation to constant temperature differences ΔT . (Grey: Voltage; Black: Power; Dotted: Progression of MPP) [21]

As P_{max} , V_{MPP} and R_{int} vary with temperature, a closed-loop control of I_{load} is necessary, to maintain the TEG in maximum power point operation. Devices which shift the operating point of the TEG devices to the MPP are called maximum power point trackers (MPPT). MPPT continuously adjust the load current to extract the maximum power available from the TEG.

MPPT-algorithms

The most commonly used MPPT algorithms are Perturb & Observe (P&O), Incremental Conductance (INC) and fractional open-circuit control which were originally developed for PV-systems. P&O and INC require the measurement of both voltage and current presenting a computational overhead, whereas the fractional open-circuit algorithm only needs a voltage reading in conjunction with less computation.

The normal P&O technique is based on continuously perturbing the electrical operating point, measuring the outcome and comparing the computed power to its previous value. There are two main drawbacks of this method: in thermal steady-state an effect known as Limit Cycle Oscillation (LCO) occurs. The electrical operating point oscillates around the MPP due to the continuous perturbation and adjustment. Moreover it cannot be guaranteed to find the MPP during rapid thermal transients.

INC algorithm computes the derivative dP/dI , which is smaller than zero to the left, greater than zero to the right and zero at the MPP. Consequently the instantaneous conductance compared to the incremental conductance yields the MPP. This method has the advantage over P&O that it can determine when the MPP is reached.

The normal fractional open-circuit technique has the main disadvantage that the TEGs are normally disconnected from the load at regular intervals to allow the converter's input capacitor to sample and hold V_{OC} . During the sample and hold time no power can be harvested but more importantly reconnecting the load to the TEGs results in switching losses and (interrupts the normal operation of the converter by) transient events. As well the Peltier effect on temperature is not considered. Furthermore the sample and hold time may be as long as hundreds of μs .



The fractional open-circuit algorithm used by the British company Thermolectric Conversion Systems Ltd. (TCS, <http://www.teconversion.com/>) uses an innovative technique overcoming these drawbacks and therefore was applied for the Powerstep pilot. By omitting the input capacitor time constant this approach is considerable faster. While measuring V_{oc} the TEG is operated in load condition, still providing power (with the converter in a pseudo-normal state) hence the Peltier effect acting on the temperature is factored in. An additional benefit is that the fractional open-circuit algorithm always finds the MPP in both thermal equilibrium and fast transient conditions.

Distributed vs. centralized MPPT

The term Distributed MPPT (DMPPT) refers to the decentralized operation of several MPPT trackers in on system and opposes the usage of only one large single MPPT unit. In case of the TEG it was decided to use one MPPT for each TEG-unit. This allows for a more robust operation and increases the system efficiency by avoiding circuit losses. Moreover it helps to maintain voltage and current in a reasonable range.

Energy buffering

As both the supply side (represented by the thermoelectric system) and the demand side (represented by the load e.g. electrical grid or a machine) are fluctuating over time the energy provided by the TEG has to be buffered in conventional DC battery. Typical battery sizes for applications like the CHP in Braunschweig are in the range of 2.000Ah, when using 12V systems. In order to charge the battery, a specific battery management circuit has to be deployed.

Connecting to grid

For connecting the TEG power to the electric grid, electrical alternators have to be deployed. The components are standard in photovoltaic industry.

Some electrical requirements of the TEG are given by legislation in accordance with IEC 60449, DIN EN 50110-1:2014 (EN 50110-1:2013) and DIN EN 50110-2:2011 (EN 50110-2:2010). By keeping internal electrical DC voltages below 50V a safe operation can be ensured.

3.2.4. TEG integration in Braunschweig

The integration of the thermoelectric generator to the Braunschweig site was based on a reduced TEG assembly with a total of 9 heat exchangers, 12 coolers and 72 TE modules ($40 \times 40 \text{ mm}^2$) as shown in Figure 16. The reduced version was chosen because of budget constraints and to allow easy installation. The scaling factor applied was 1:10, using a single stage equipped with commercial Bi_2Te_3 modules.





Figure 16: Thermoelectric generator prototype for Braunschweig case study

The electrical concept utilized a distributed MPPT scheme to achieve an effective system with a low number of MPP-trackers. Instead of using an individual MPPT for each module, the 8 modules of one TE-unit are grouped into a serial/parallel configuration as illustrated in Figure 17. The 2x2 TEM arrays connected in serial configuration are physically located on top and bottom of the heat collector, ensuring electrical compliance in open circuit voltage and at the same time minimizing parasitic currents due to high symmetry.

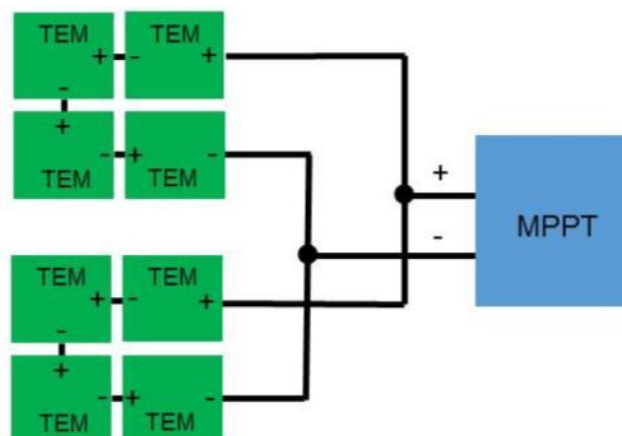


Figure 17: Interconnection model of employed TEM arrays

A total of nine TE-units and MPPTs are interfaced to a voltage and current (VI) monitor, bundled and housed by the backplane (Figure 18). The power generated by the TEG is used to charge a battery bank. Excessive power is dissipated by a switchable electronic load.



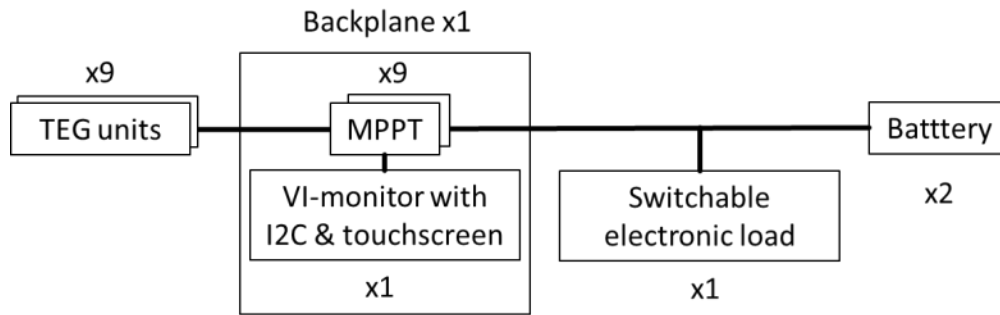


Figure 18: Electrical concept for power generation and storage

For installing the TEG at Braunschweig, a safety concept had to be developed that allows to monitor operation and mitigate critical situations. The following points have been identified during the analysis:

Table 6 Risk analysis and mitigation (operation phase)

Identified Risk	Criticality	Detectability / Means	Mitigation
Cause high backpressure on exhaust line - System failure - Leakage	High	High - Monitoring of exhaust gas backpressure	Operate in parallel configuration; Connect directly to chimney
Leakage of hot exhaust gas (500°C) - Fire, burns - Accumulation of CO, CO ₂	High	Medium/Low - CO-Sensor - Monitoring of exhaust gas backpressure	Forced room ventilation Close gas-safety valve in case of threshold violation: - CO to high - Backpressure to low
Leakage of coolant (80°C) - Burns - System failure	Medium	High - Monitor flow rate	Close gas-safety valve; close coolant valves; stop pump; A pressure relief valve is needed in case of overheating
Failure of TEG cooling system - Damage to TEG - Damage to hoses	Medium/Low	High - Monitor flow rate	Close gas-safety valve; close coolant valves; stop pump; A pressure relief valve is needed in case of overheating
Electrical failure of load - Fire	Medium/Low	High	Use CE-tested electronic load; Deactivate circuit in case of overvoltage

From the analysis, the need for a gas and coolant safety shut-off valves as well as a general system monitoring was identified. It was decided to operate the TEG in a parallel configuration to the existing heat exchanger and to connect it directly to the chimney of the CHP plant to avoid excessive backpressure. Figure 19 shows the integration of the TEG into the existing CHP system.



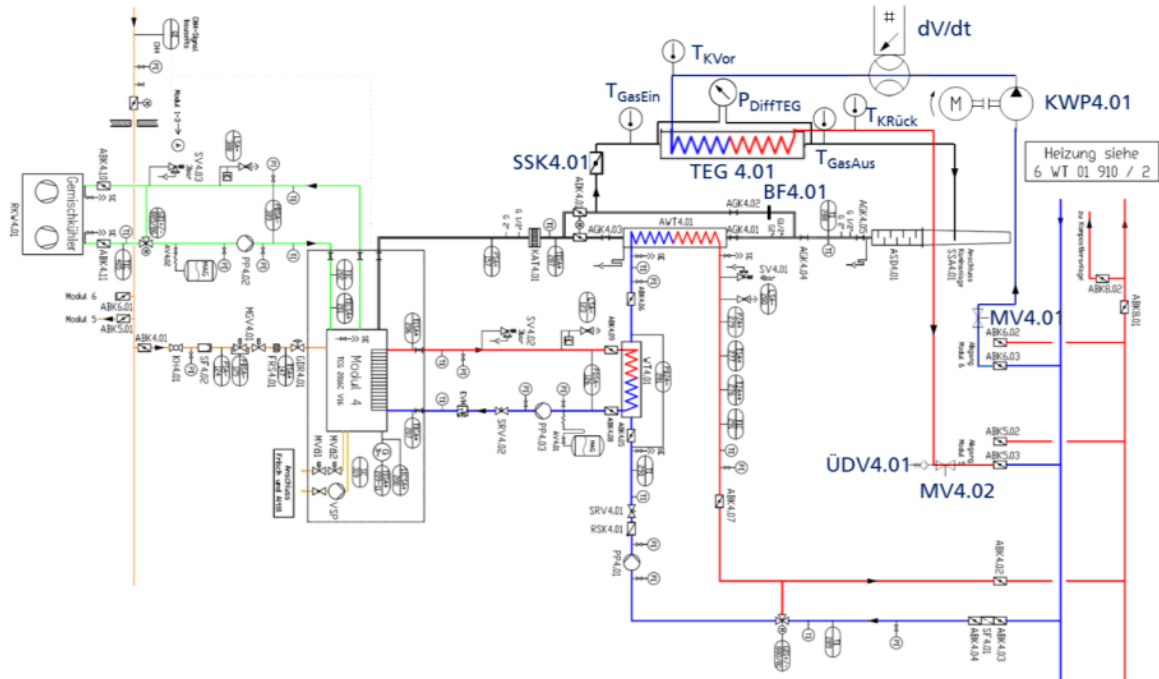


Figure 19: TEG Installation scheme

The shut-off valve for gas (SSK4.01) is used to disconnect the thermoelectric generator (TEG4.01) from the hot exhaust gas. It is located on the switchable bypass of heat exchanger (AWT4.01), directly after the catalyst (KAT 4.01). After exiting the TEG the cold exhaust gas is directly fed into the chimney of the plant.

The TEG coolant is extracted from the CHP remote heating return line using an auxiliary pump (KWP4.01) and later re-injected into the same line in a downstream position. This allows using a partial volume flow of coolant and thus allows managing the backpressure and volume flow on the TEG coolers. The TEG coolant circuit can be independently fully disconnected by closing the valves MV4.01 and MV4.02. In case of boiling of coolant, the valve (ÜDV4.01) will open once a maximum pressure of 3 bar is exceeded.

The sensors installed monitor the volume flow of coolant (dV/dt), the differential gas pressure across the TEG heat exchangers ($p_{Diff,TEG}$) as well as several temperatures.

As shown Figure 20, the data acquisition system is based on a Raspberry PI with Linux operating system. Sensors are interfaced through USB measurement cards. A Raspberry Pi B3 is used as central control of the measuring system and to display data. It also interfaces to the MPPT system (Figure 18) and stores all data on a local USB drive. The acquisition system is mounted inside a standard 19 inch electronics rack (Figure 21).

Remote servicing is enabled by using a UMTS modem to connect the measurement system to the internet. Measurement data is periodically synchronised with an FTP-Server at Fraunhofer.



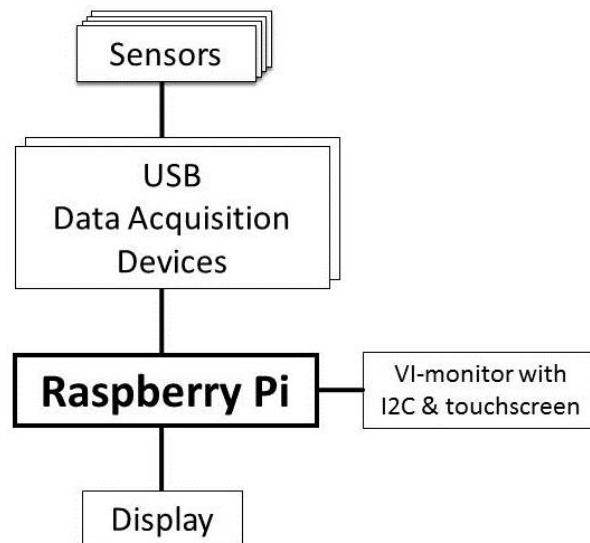


Figure 20: Schematic of measurement system with Raspberry Pi as central control unit.



Figure 21: Measurement system with Raspberry Pi B3 single board computer. Left: Front panel, Right: Internal wiring

3.3. Manufacturing and lab testing

3.3.1. Manufacturing

The manufacturing of the TEG comprises several process steps.

1. Incoming inspection: Purchased components are inspected for defects. Special focus is set on heat collectors, coolers and TE-modules. TE-modules are electrical-ly characterised for ZT performance and resistance as well as for module height.
2. Stacking: During the stacking process, alternating layers of coolers, TE-modules and heat collectors are configured. Great care has to be taken on a clean work environment, as larger particles could degrade the thermal contact between the components. The thermal interface material is graphite.
3. Compressing: Stacks are compressed to achieve a force fit and good thermal contacts.

4. Cooling harness – vertical: The vertical distribution of coolant lines is assembled by using bracing technology. The joining process is followed by a pressure/leakage test.
5. Wiring - vertical: The vertical electrical wire harness is built. Great care has to be taken not to touch elements that heat above $> 200\text{ }^{\circ}\text{C}$ during operation. It is completed by electrical test.
6. Functional test on hot air bench: All TE-units are functionally tested with hot air (see next chapter).
7. Mounting on rack: The TE-stacks are mounted on the mounting frame.
8. Cooling harness – horizontal: Horizontal coolant distribution and interface piping. Assembly is again followed by a leakage/pressure test.
9. Mounting of exhaust inlet/outlet cones. Pressure testing.
10. Wiring – horizontal: Horizontal cabling, attachment of connectors. Final electrical test.

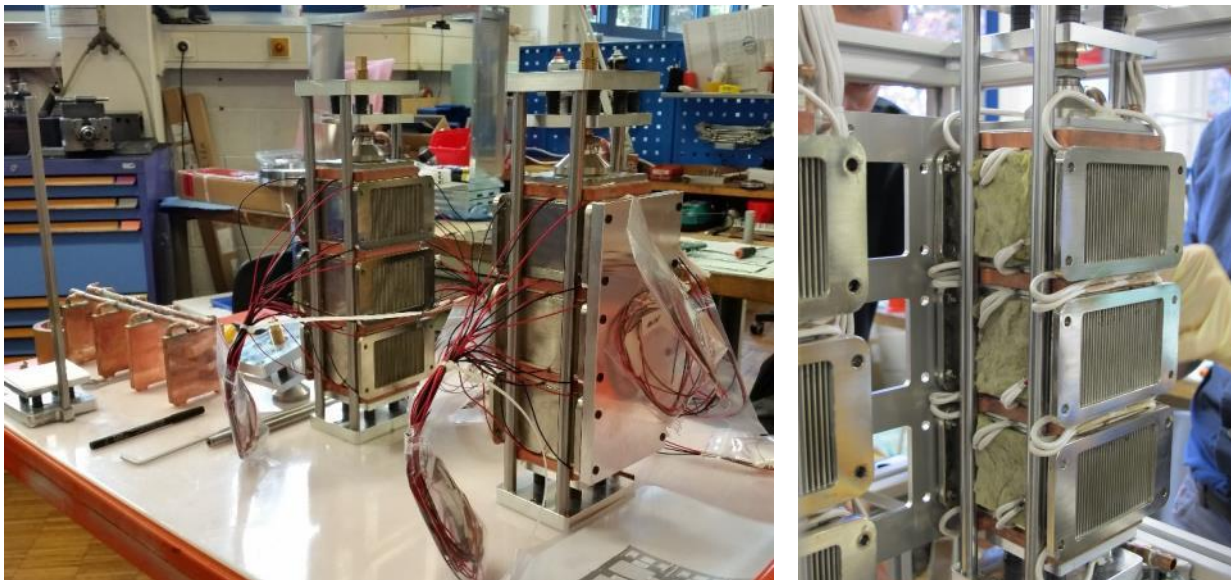


Figure 22: Manufacturing of TEG. Left: TE-unit stacks before bundling the wire harness, Right: Mounting of TE-stacks on the rack

3.3.2. Lab testing of the TEG-unit stacks

Prior to delivering the TEG to the WWTP/CHP in Braunschweig the individual TEG-units were tested on a hot air test bench (Figure 23). The TEG-units of the three stacks were tested successively under quasi-static operating conditions with air inlet temperatures of about 450 to $485\text{ }^{\circ}\text{C}$ and air mass flow rates of about 40 to 75 kg/h (design operating point: 44 kg/h , $450\text{ }^{\circ}\text{C}$) using Fernox Solar S1 as coolant (flow rate 10 l/min). All relevant parameters of the air stream and cooling cycle were recorded. The power output of the TEG-unit was measured using a maximum power point tracker (MPPT) following the electrical circuit setup as described in section 3.2.4 (Figure 17). Additionally, the surface temperature on one side of the heat collectors was measured on four measuring points close to the TE modules to record an estimate of the hot side temperature of the TE-



modules (the procedure was repeated during the field tests in Braunschweig for comparison).

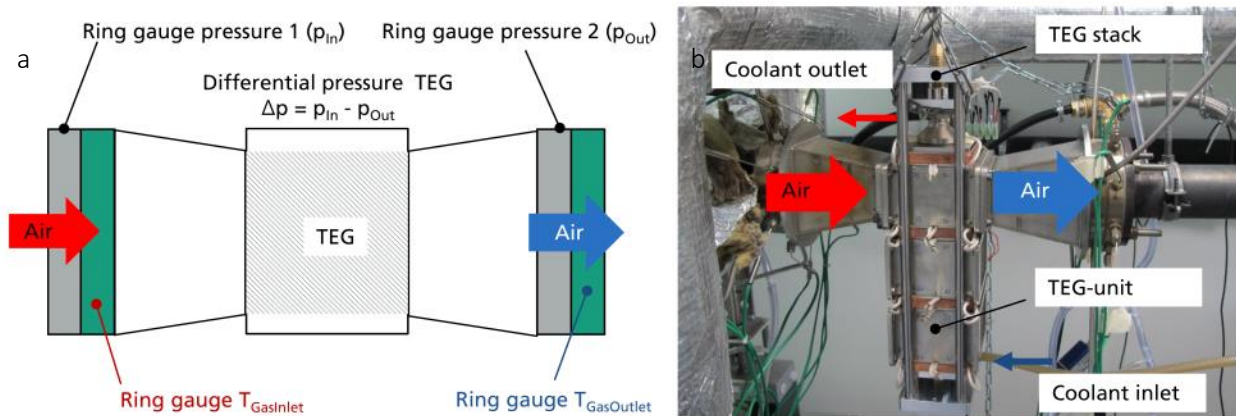


Figure 23: Experimental setup hot air TEG test bench. (a) Sketch of the measurement setup. (b) Image of a TEG stack tested on the hot air test bench at Fraunhofer IPM.

For a coolant temperature T_c of 20 °C the power output of the TEG-units ranged in between ~73 to ~100 $W_{el, TEG}$ and increased in relation with the air temperature and the mass flow rate (Figure 24). Both an increase of the air temperature or the mass flow rate led to higher mean surface temperatures on the side of the heat collector and the differential temperature over the TE-modules. In comparison under otherwise the same operating conditions the power output of the TEG-units dropped by about 21% when T_c was increased from 20 °C to 60 °C (Figure 25). For the design operating point ($T_{Air, in}=450$ °C, $\dot{m}_{Air}=44$ kg/h) the mean power output of the TEG-units was (76 ± 2) $W_{el, TEG}$ for $T_c=20$ °C (Figure 24) and (61 ± 1) $W_{el, TEG}$ for $T_c=60$ °C.

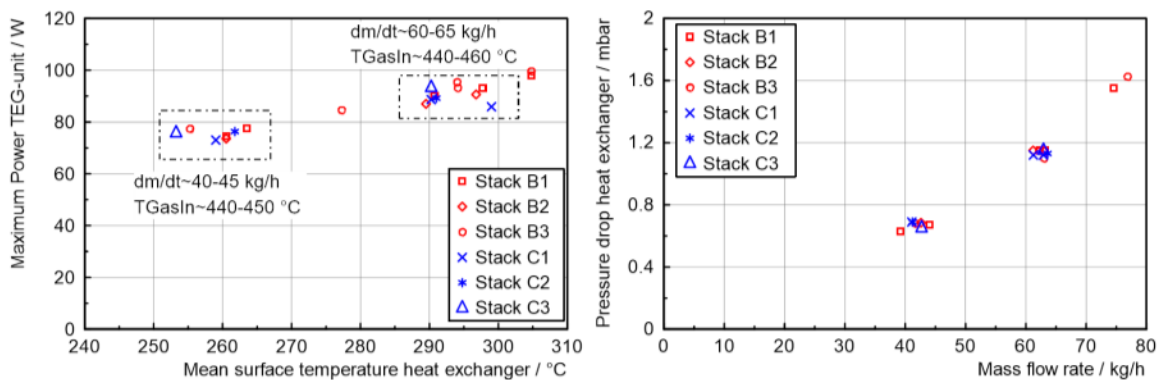


Figure 24: Comparison of the power output of a TEG-unit and the differential pressure over the heat exchanger for stack B and C for a coolant inlet temperature of 20 °C and a gas inlet temperature of about 450 °C (hot air test bench at Fraunhofer IPM).

Independent of the coolant temperature the pressure drop over an individual TEG-unit was below 2 mbar for mass flow rates lower than 80 kg/h and about 0.7 mbar for mass flow rates in between 40 to 45 kg/h.



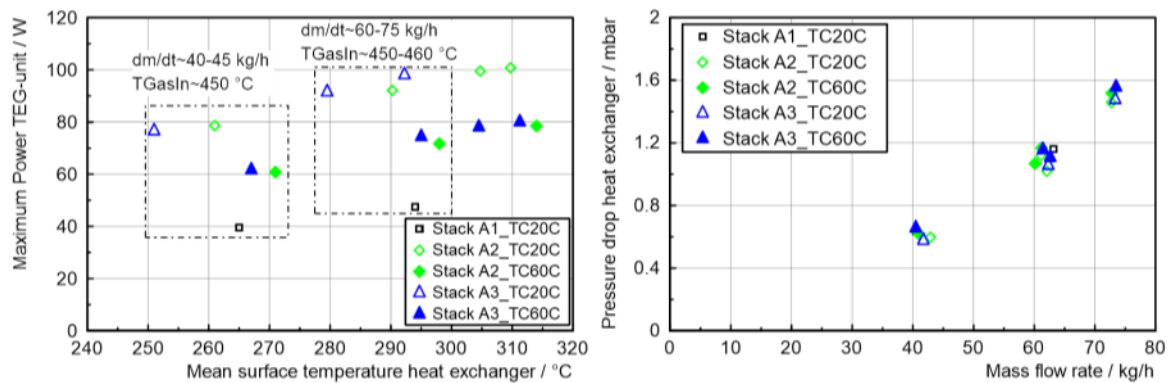


Figure 25: Comparison of the power output and differential pressure of the TEG-unit for stack A for a coolant inlet temperature T_c of 20 °C and 60 °C and a gas inlet temperature of about 450 °C up to 485 °C (hot air test bench at Fraunhofer IPM).

The efficiency of the TE-modules when integrated into the heat exchanger was calculated based on the electrical power output of the TEG-unit and the heat flow rate to the coolant for quasi-static conditions ($\eta_{\text{TEG-module}} = P_{\text{el,TEG-unit}} / (P_{\text{el,TEG-unit}} + \dot{Q}_{\text{Coolant}})$) (Table 7). It should be noted, that due to a coolant inlet temperature of 20 °C, the module efficiency is higher than in the final application with 60°C to 80°C.

Table 7: Summary of hot air test bench measurements for TEG stacks A-C.

Mass flow rate air [kg/h]	Mean power output TEG-unit [W_{el}]*	TEG module efficiency [%]*
~40 - 45	76 ± 2	$4,09 \pm 0,08$
~60 - 65	91 ± 2	$4,3 \pm 0,1$

Gas inlet temperature : ~450 - 460 °C, coolant inlet temperature: 20 °C;
 *without TEG-unit A1; one standard deviation (SD)

3.4. Field deployment test

3.4.1. Installation of TEG in the exhaust system of the CHP

As mentioned in 3.2.4 the installed TEG was designed to use about 10 % of the total available exhaust gas mass flow rate of the CHP. To increase the flexibility of the CHP operation and to avoid the risk of having a too high back-pressure, the TEG was integrated in a bypass configuration parallel to the standard heat exchanger (Figure 26). This allowed controlling the exhaust gas mass flow rate through the TEG by changing the position of a by-pass valve ① (Figure 26) upstream of the standard heat exchanger ② (Figure 26) and the TEG. When set in positions in between 0 % and 100 % the resulting mass flow rates to the TEG and the standard heat exchanger depends on the resulting backpressures building up in front of the units.



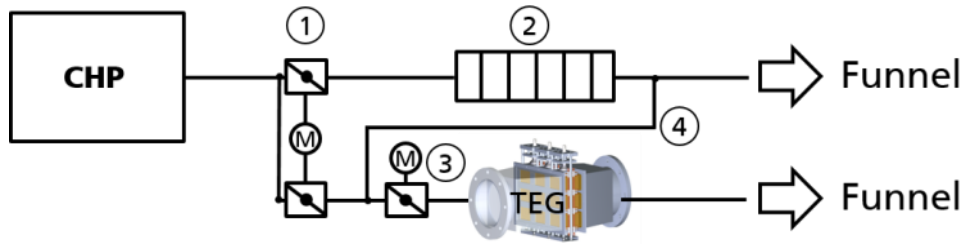


Figure 26: Simplified sketch showing the integration of the TEG in the exhaust system of the CHP.
 1: By-pass valve, 2: standard heat exchanger, 3: rapid-action valve, 4: by-pass line for standard heat exchanger.

Steel pipes with a diameter DN200 were used as exhaust pipes leading to the TEG and from the TEG to the funnel (Figure 27). In order to be able to cut-off the exhaust gas supply to the TEG in case of an emergency a rapid-action valve was integrated before the TEG ③ (Figure 26). To reduce heat losses from the main exhaust pipe to the TEG the piping was covered with a layer of insulation (thickness 100mm).



Figure 27: Overview of the TEG with electronic control unit/measurement electronics. 1: TEG; 2: electronic rack with MPPTs, electronic load, data acquisition unit; 3: coolant pump; 4: rapid-action exhaust gas valve; 5: main exhaust pipe of standard heat exchanger by-pass; arrows indicate the flow direction of the exhaust gas (photo taken 07.11.17).

3.4.2. Results of field tests

After integration of the TEG, four field tests were conducted with the aim to determine the typical performance output of the TEG and in order to learn more about the operation in application CHP (see Table 8 for details on the tests). As previously explained, the aim was to use about ten percent of the total exhaust gas mass flow rate.

Table 8: Overview of the conducted field tests

Field test	Date	Summary
0	16.-19.10.17	System installation
1	06.-07.11.17	First commissioning attempt: DCDC converters failed upon start-up of TEG, open- and short circuit measurement performed
2	27.-29.11.17	Repair of power electronics: successful testing of the TEG with running power electronics (DCDC converters, electronic load). Failure of data acquisition system.
3	10.-22.01.18	Repair of data acquisition system. 24h test run (partially) with power electronics. 10-day continuous test run with active exhaust. Failure of power electronics and data acquisition system.
4	29.-31.01.18	24h test run (partially) with updated power electronics. Decommissioning of TEG.

In the field deployment, the mass flow rate \dot{m} of the exhaust gas through the TEG could not be measured directly. Instead, it was derived from the coolant heat flow rate $\dot{Q}_{Coolant}$ and the el. power output of the TEG $P_{el,TEG}$ using the following equation:

$$\text{Equation 16 } \dot{m}_{ExhaustGas} = \frac{\dot{Q}_{Coolant} + P_{el,TEG}}{\Delta T_{ExhaustGasTEG} * \bar{c}_{pExhaustGas}},$$

where $\Delta T_{ExhaustGasTEG}$ stands for the measured temperature difference of the exhaust gas occurring over the TEG and $\bar{c}_{pExhaustGas}$ for the mean specific heat capacity of the exhaust gas.

This method is based on the assumption that no significant heat losses occur from the TEG to the environment. To minimize heat losses the inlet cones of the TEG and part of the heat collector surfaces were insulated with rock wool. Nevertheless, since the heat losses cannot be fully avoided, the mass flow rates obtained using Equation 16 are likely underestimated. This results from measuring the exhaust gas temperatures before the inlet and outlet cone of the TEG. Due to heat losses the effective temperature drop of the exhaust gas over the TEG-unit heat collector is lower than over the complete system. Moreover, inaccuracies in the determination of the mean gas temperatures and parasitic heat transfers to the coolers also leads to errors in the measurement of $\dot{Q}_{Coolant}$, which also affects the calculated mass flow rate of the exhaust gas. The overall deviation can be assumed to be around 30 to 40 %.

On 28.11.2017 the TEG was tested with electrical load and under three different operating conditions (Figure 28). By changing the position of the by-pass valve (Figure 26, 1) the mass-flow rate and the temperature of the exhaust gas were varied. The valve was set to 25, 50 and 75 % (the exhaust gas mass-flow rate through the TEG increased with higher percentage values).



Measurement: 28.11.17, SE|BS, TCoolantIn: ~60 °C [TEG MPPT]

Save time: 08.12.2017 09:23:01.0000

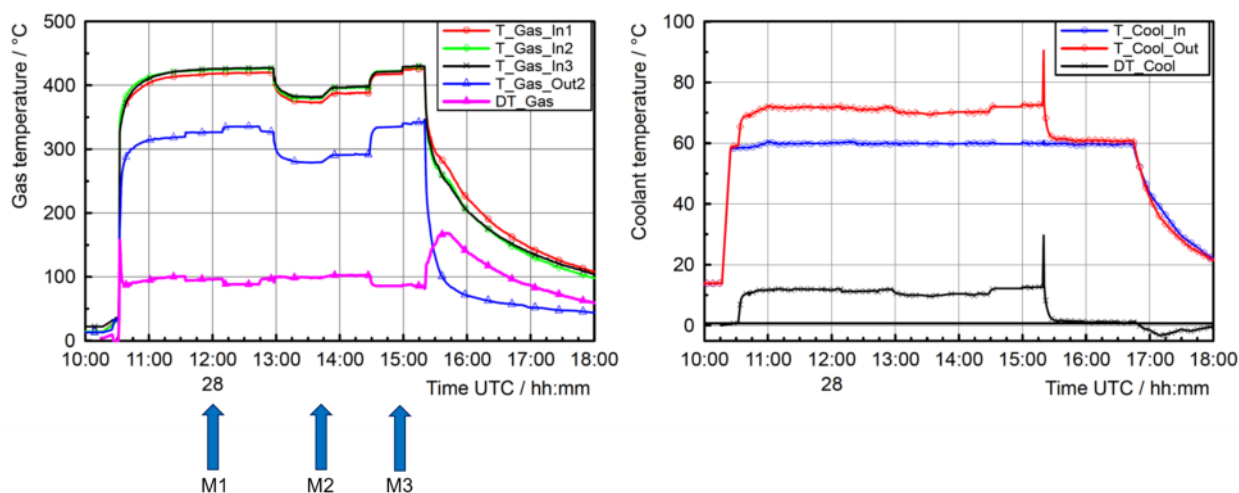


Figure 28: Overview of the gas and coolant temperatures during field-test 2 (the indices mark the time of the taken measurements). M1: bypass-valve setting: 50 %, M2: bypass-valve setting: 25 %, M3: bypass-valve setting: 75 %.

During the test each of the nine TEG-units produced between about 23 to 68 $W_{el,TEG}$ for the different operating points (Figure 29). In total the TEG delivered an electrical output power of about 400 to 530 $W_{el,TEG}$. The TEG-unit A1 was running at 50% power, as only one TE-module array of this unit was functional after assembly of the complete system³. When neglecting this defect, the following mean power outputs for the TEG-units were obtained using maximum power point tracking (Figure 29b): M1: $58 \pm 3^4 W_{el,TEG}$; M2: $46 \pm 3 W_{el,TEG}$; M3: $62 \pm 3 W_{el,TEG}$. Overall, the standard deviations within the 8 TEG-units were about 5% of the mean values. Hence, the deviation of the electrical power output of the different TEG-units was rather low which indicates that the differential temperatures over the TEG-units were similar.

The result shows that the TEG design enabled a homogeneous distribution of the flow through the individual TEG-units.

³ One module array was mechanically broken during re-work of a cooler after detection of a leak during lab test.

⁴ One standard deviation

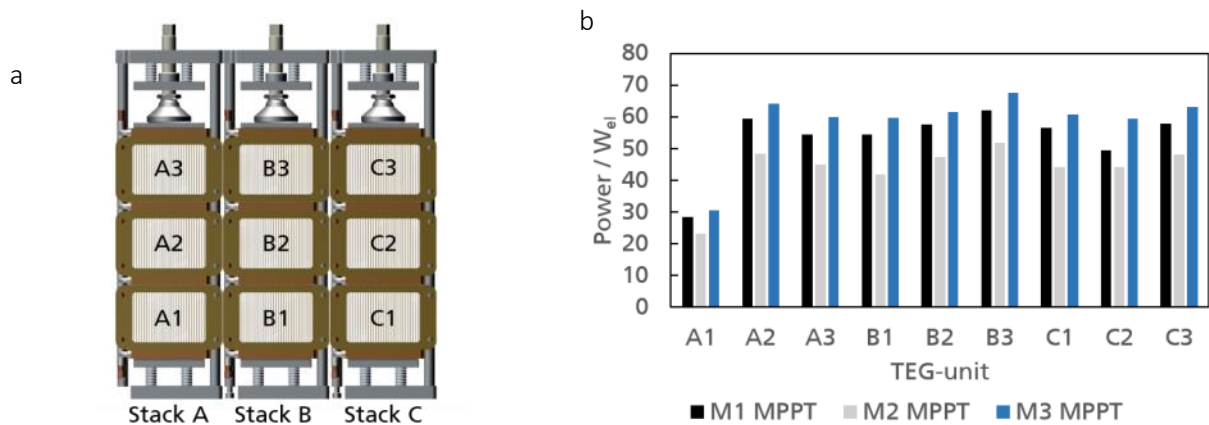


Figure 29: Maximum electrical power outputs of the TEG-units during field-test 2. (a) CAD image showing the location of the TEG-units in stacks A-C, (b) Comparison of measurements conducted with the usage of maximum power point trackers (MPPT). M1: by-pass valve set to 50 %, M2: 25 %, M3: 75 %. M2 lowest mass flow rate of exhaust gas, M3: highest mass flow rate. In total, depending on the operating conditions the TEG delivered an output power of about 400 to 530 $W_{el,TEG}$.

For details on the operating conditions and experimental results, see Table 9.

Table 9 Detailed results of field test 2. (Note: Module A1 delivering 50% of typical power)

M	Electrical Power Engine	Valve setting By-Pass	T_{gasIn} Mean	T_{gasOut} Mean	$T_{coolantIn}$	Heat flow rate to coolant	Calculated mass flow rate gas	Δp_{Gas}	Total Power output TEG
	(kW)	(%)	(°C)	(°C)	(°C)	(kW)	(kg/h)	(mbar)	(W)
1	680	50	423	322	60	17,3	549	1,7	488
2	680	25	393	286	60	14,6	442	1,2	394
3	680	75	427	336	60	18,1	640	2,5	527

The maximum power observed during the test was 527 W_{el} . Field test number 3 and 4 showed comparable results.

3.4.3. Lessons learned from field testing

The field deployment of the TEG prototype was completed by end of January 2018. The field deployment was very helpful to improve the development of the TEG. The following paragraph gives a short summary on the lessons learned.

TEG transport and handling

Despite the prototype weight of 125 kg, the road transport to Braunschweig including loading, transport (vibrations) and the mechanical handling was without problems. The way of transportation can also be applied to a large scale TEG.



TEG installation

In the recent installation, the decoupling element was installed downstream of the TEG, with the main intention to compensate for thermal expansion. During operation however, quite significant vibration was observed on the exhaust pipe. Therefore, for the next installation, the TEG should be mounted after the decoupling element, accepting some thermal loss.

The distance from the catalyst to the TEG was about 2-3 meters; this led to a gas temperature decrement of about 50K, which corresponds to a significantly high thermal heat loss. Future TEG should be installed directly after the cat (like heat exchangers). All pipes should be insulated for safety and to avoid heat losses.

The position of the TEG should be located at an elevated point of the exhaust line to avoid accumulation of condensate (see condensation marks in Figure 30 and Figure 31). Alternatively it could be installed vertically.

The cooling line integration proved to be very robust. A large scale TEG should inject heat downstream of the engine heat exchanger.

TEG operation

During the lab tests, 3-month trial installation and operation no degradation of the thermoelectric components was observed⁵. The basic TEG functions of guiding exhaust gas and converting heat to electricity were performing constantly stable.

The rust particles that were found inside the heat exchange tube and cones after the field test in Braunschweig, as shown in Figure 30 and Figure 31, can be allocated to upstream, low grade steel pipes. The occurrence of the particles could be avoided by using a shorter, high-grade exhaust pipe.

TEG operation has to consider phases of non-operation: in industrial environment power-cuts and downtimes may happen quite often; therefore the TEG electronics should be able to survive and recover without damage.

As the remote servicing service can disconnect, all essential functions should be available on-site.

In cold condition, the accumulation of condensate inside the tubes can threaten the function of the heat collectors, therefore the TEG should be mounted in elevated position, with the possibility to drain liquid.

The power electronics still have to be improved for stability and battery management capability and for interfacing to the power grid. Backpressure monitoring has to consider system vibration and noise in industrial environment.

⁵ Except for one module array in TEG-unit A1 that was mechanically broken during re-work of a cooler after detection of a leak during lab test.



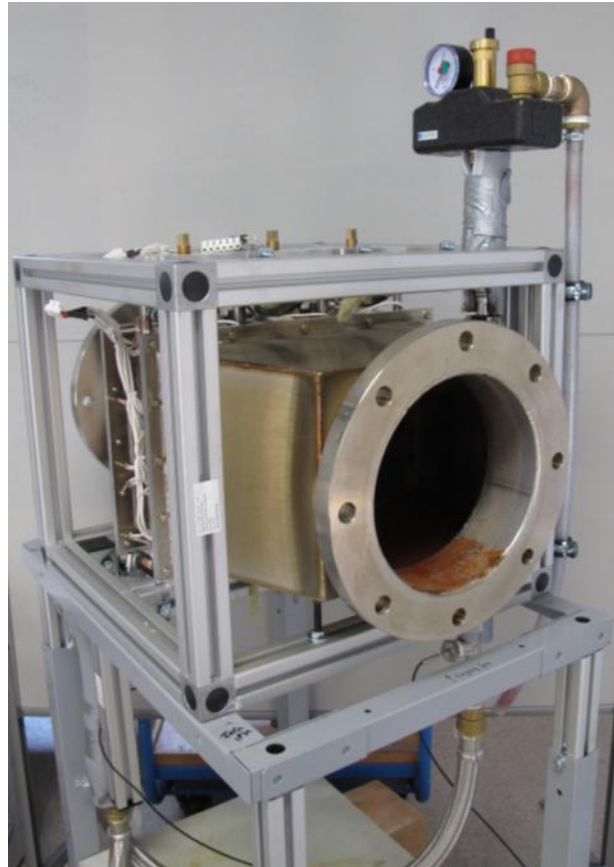


Figure 30: TEG prototype after decommissioning

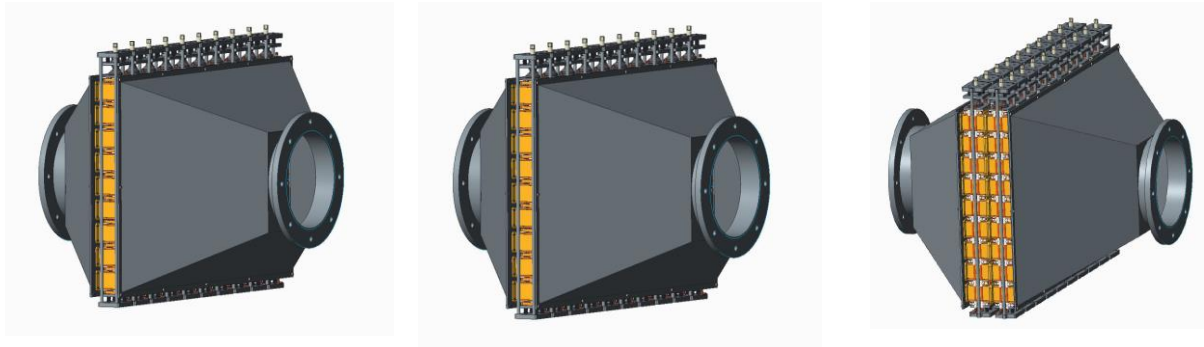


Figure 31: Heat exchange tubes inside the TEG with condensation and rust particles from upstream pipes.

3.5. Projected full-scale performance of TEG

The projected power output of a full-scale system was calculated by increasing the number of TEG-units under the assumption of a linear scaling with mass flow. Three different full-scale TEG-designs were evaluated:





1. TEG with single converter stage based on low-cost TE-modules (90 TEG-units)
2. TEG with single converter stage based on high performance TE-modules (90 TEG units)
3. TEG with two converter stages (two heat collectors/TEG-units in series) based on high performance TE-modules (180 TEG units)

Figure 32: TEG systems for full scale performance calculation

The performance data for the full-scale calculation was based on test bench results and not on the field tests. This can be justified as follows:

1. The TEG position during field deployment was not representative for a final system. The inlet gas temperature in the position was about 20 to 30 K lower due to long distance between TEG and engine (approx. 2-3m).
2. The mass flow rate was only measured indirectly; this results into a high relative error (as explained in chapter 3.4.2).

The methodology and different steps applied to calculate the projected power output of the different TEG-designs are summarized in Figure 33.

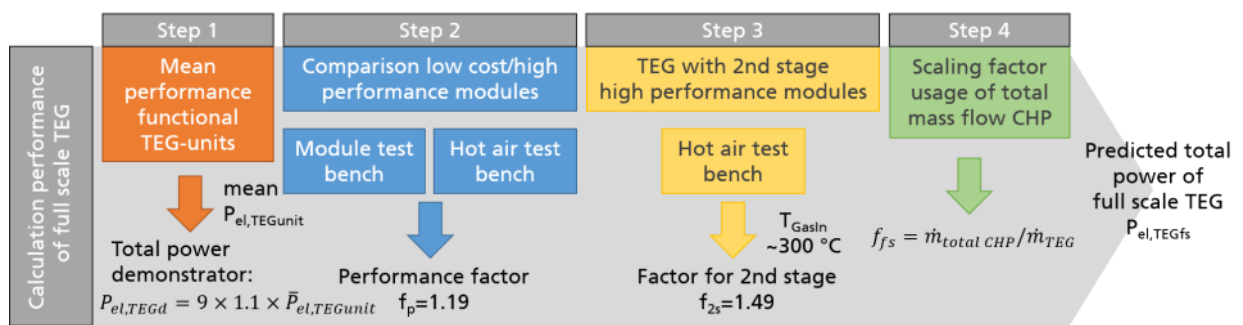


Figure 33: Steps used to calculate the full-scale performance of a high performance TEG based on test bench measurement data (with $T_{GasIn}=450\text{ }^{\circ}\text{C}$).

Step 1:

The prototypes comprised one defective TE-unit. This unit was excluded from calculating the representative average power per TEG unit in the respective working condition (60 °C/450 °C). The remaining 8 units were used to calculate the mean power output. To accommodate for the power loss caused by increased coolant temperature, the bench test power output values of six TEG-units were reduced by 21 %. (see chapter 3.3



for a comparison of the output power at 20 °C and 60 °C coolant temperature). The resulting mean output value per TEG unit is 60 W. In order to compensate for the different specific heat values of dry air and exhaust gas, this power was multiplied by a factor of 1.1 since exhaust gas has a higher specific heat than dry air [18].

Step 2:

The performance difference of low-cost and high performance TE-modules was analyzed by conducting TE-module tests on a module test bench and TEG-unit test with hot air. The module test bench results show a performance increase of about 20 % when using high performance modules (Figure 34).

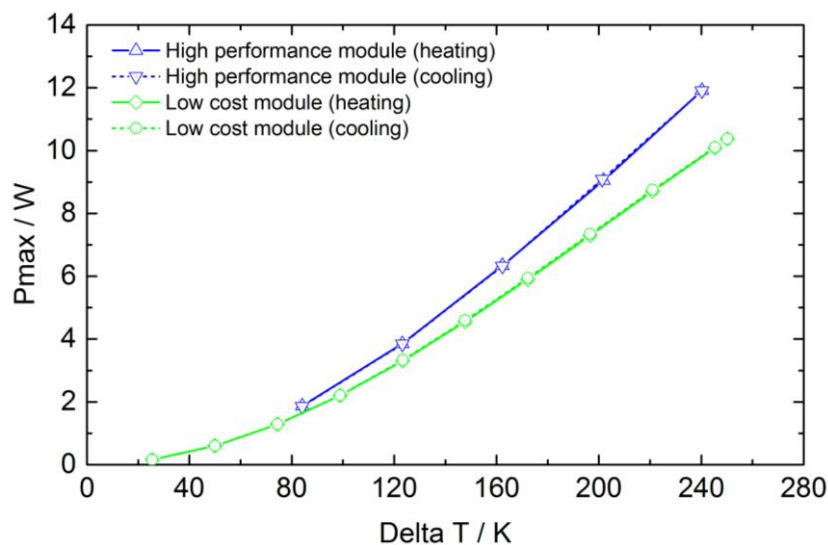


Figure 34: Performance comparison of a high performance and a low-cost TE-module on a module test bench ($T_{\text{coolant}} = 75 \text{ }^{\circ}\text{C}$). At $\Delta T = 240 \text{ K}$ the low cost module delivered ~10W and the high performance module ~12W which corresponds to a 20 % higher performance.

The performance factor was confirmed with the hot air test bench results. A TEG-unit equipped with eight high performance modules was compared with a TEG-unit comprising eight low cost TE-modules under similar operating conditions (Figure 35). Overall, taking into account all conducted measurements at a coolant inlet temperature of 20 °C and 60 °C, the mean performance increase was about 19%. The factor was used since it is a little more conservative than the factor obtained for 60 °C only (19 % vs. 21 %). The power output was plotted over the logarithmic mean temperature difference of the counter flow heat exchanger [18]. This takes into account the non-linear temperature progression of the hot air stream and the coolant stream over the length of the TEG-unit/heat exchanger.



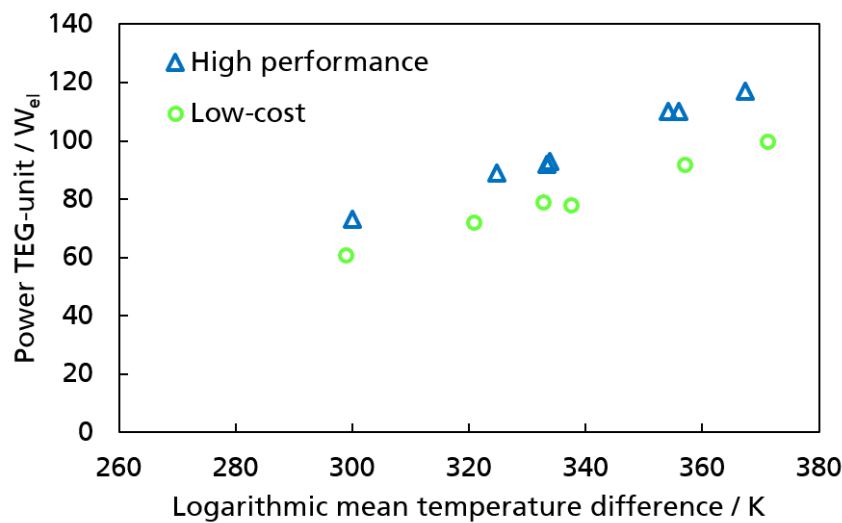


Figure 35: Performance comparison of a high performance and a low-cost TE-module on a hot air test bench ($T_{coolant} = 20\text{ °C}$ and 60 °C). Overall, the mean increase in power for high performance vs. low-cost modules was about 19 %.

Step 3:

Hot air tests conducted with a decreased air temperature of about 310 °C were performed to simulate a second TEG stage. For the experiments, the TEG-unit was equipped with eight high performance modules. The increase of power was calculated by summing up the power output of stage 1 and stage 2. Using two TEG stages with high performance modules leads to a power increase of about 50 % (Table 10).

Since the inlet air temperature was higher than the outlet temperature of stage one for a mass flow rate of about 45 kg h^{-1} (about 25 K), this represents an optimistic estimate of the power increase.

Table 10: Performance result of simulated two stage design.

Stage	Masse flow rate (kg h ⁻¹)	T _{Gasl} n (°C)	T _{Gas} Out (°C)	T _{coolant,in} (°C)	Heat flow rate coolant (W)	Power TEG-unit (W _{el})	Heat transfer efficiency	η _{TEG-module}
1	40-50	454	275	20	1751	92	41%	5,0%
1	60-70	454	311	20	1960	110	33%	5,3%
1	40-50	452	285	60	1807	73	42%	3,9%
1	60-70	459	323	60	2085	89	34%	4,1%
2	40-50	311	194	20	1227	45	40%	3,6%
2	60-70	313	221	20	1357	57	31%	4,0%
2	40-50	313	204	60	1296	34	43%	2,6%
2	60-70	316	231	60	1345	42	33%	3,1%
1+2	40-50	454	194	20	2978	138	60%	4,4%
1+2	60-70	454	221	20	3316	166	54%	4,8%
1+2	40-50	452	204	60	3103	107	63%	3,3%
1+2	60-70	459	231	60	3430	131	57%	3,7%



Step 4:

In the final step a full-scale scaling factor was applied. The full scale assembly comprises out of 90 (single stage) or 180 (double stage) TEG-units. The upscaling factor is in line with the mass flow increment from 44 kg/h for one TEG-unit to 3.944 kg/h for the full TEG.

Projected performance of TEG using total mass flow rate of CHP:

Applying all four steps yields the full scale performance of the TEG (Equation 17).

$$\text{Equation 17 } P_{el,TEGfull} = \bar{P}_{el,TEGunit} \cdot f_{units} \cdot f_{exg} \cdot f_{2ndstage} \cdot f_{fs}$$

where $\bar{P}_{el,TEGunit}$ stands for the mean power output of the TEG-unit at a coolant inlet temperature of 60 °C, f_{units} for the number of TEG-units used for the demonstrator TEG, f_{exg} for the increased specific heat value of exhaust gas compared to dry air, $f_{2ndstage}$ for the performance increase when using two TEG stages (two TEG-units in series) and f_{fs} for the scaling factor of the TEG (number of TEG-units required to make use of the complete mass flow rate of the CHP).

In case of the high performance TEG with two TEG stages the electrical output power is about 11 kW (Table 11). This leads to an increase of the electrical efficiency of the CHP from 41.5 % to 42.1 % (relative increases of about 1.5 %). Since the exhaust gas temperature after the TEG is higher than for the standard heat exchanger (200 °C vs 180 °C) more thermal energy remains in the exhaust gas. In addition, part of the available thermal energy is converted to electrical energy (output of TEG), so consequently the thermal efficiency of the CHP decreases. As a result, the total the efficiency of the CHP would also decrease slightly by about 1.3 %. This effect could be avoided by adding an additional small heat exchanger, or by fine-tuning the TEG system.

Table 11: Projected performances of the TEG configurations for exhaust gas mass flow rate of about 3 944 kg/h and an inlet gas temperature of 450 °C.

Efficiency CHP+TEG		relative change compared to standard design
Efficiencies CHP (current design with standard heat exchanger)		
$\eta_{Mechanical}$	42.9%	
$\eta_{Electrical}$	41.5%	
$\eta_{Thermal}$	39,7%	
$\eta_{Total} (\eta_{Electrical}+\eta_{Thermal})$	81,2%	
a) Demonstrator full scale (one stage), $P_{el,TEGfs}$	6 kW	
$\eta_{Mechanical}$	42.9%	
$\eta_{Electrical}$	41.9%	+0.8%
$\eta_{Thermal}$	32.3%	-18.7%



$\eta_{\text{Total}} (\eta_{\text{Electrical}} + \eta_{\text{Thermal}})$	74.2%	-8.7%
b) High performance demonstrator full scale (one stage), $P_{\text{el,TEGfs}}$		
$\eta_{\text{Mechanical}}$	42.9%	
$\eta_{\text{Electrical}}$	41.9%	+1.0%
η_{Thermal}	32.2%	-18.8%
$\eta_{\text{Total}} (\eta_{\text{Electrical}} + \eta_{\text{Thermal}})$	74.2%	-8.7%
c) High performance demonstrator full scale (two stages), $P_{\text{el,TEGfs}}$		
$\eta_{\text{Mechanical}}$	42.9%	
$\eta_{\text{Electrical}}$	42.1%	+1.5%
η_{Thermal}	38.0%	-4.2%
$\eta_{\text{Total}} (\eta_{\text{Electrical}} + \eta_{\text{Thermal}})$	80.2%	-1.3%

The configuration of using a two stage design combined with high performance modules (c) results into an increase in electrical yield of about 1.5 %.

3.6. Projected TEG system price

The cost of a system can be split into several cost components, depending on the life cycle of the system. Different aspects can become relevant: materials costs, manufacturing costs, installation costs, operating costs, maintenance costs, decommissioning costs and disposal/recycling costs.

As the TEG system is not yet established in production and operation, the analysis in this chapter focuses mainly on the aspects of material and manufacturing costs as well as operation and maintenance costs. Other cost items (installation, decommissioning, and disposal) are deferred for this first examination.

The **materials costs** of the system are a major contributor to the system cost. They are reflected in the bill-of-purchase materials (BOM). The system boundary for this approach excludes the installation cost elements for integration of the TEG into the CHP, e.g. fluid or gas valves, a coolant pump, pipes, electrical battery and alternator. They are depending on the final integration concept.

The BOM of a TEG can be split into the following subgroups:

- **Cooling:** All part costs related to the fluidic heat extraction of the TEG. Most important the coolers, but also pipes, fittings, hoses, etc.
- **TE-Layer:** Cost of the TE-modules
- **Exhaust:** All part costs related to exhaust gas guiding and heat extraction from exhaust gas. Most important components are the heat collector tubes, but also inlet/outlet cones and flanges.
- **Electronics:** The electronics and wire harness to provide a DC power output. Including the MPPT circuit.
- **MechFrame:** The mechanical frame to support the TEG stacks.



Naturally, the cost distribution differs from the actual prototype to a full size TEG prototype to a serial TEG device. Figure 36, Figure 37, Figure 38 show the cost distributions and EUR/W relations of the BOM of the TEG systems at prototype scale and at full scale and give a tentative prognosis for a future serial production scenario.

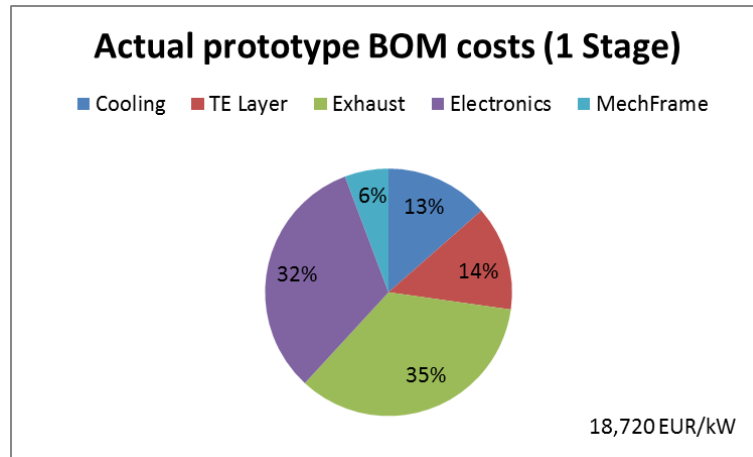


Figure 36: BOM cost split of actual POWERSTEP prototype

Figure 36 shows the cost of the actual prototype. Major cost contributors are the heat collector tubes and the electronics. The off-the-shelf TE-modules only account for 14 % of the total system costs.

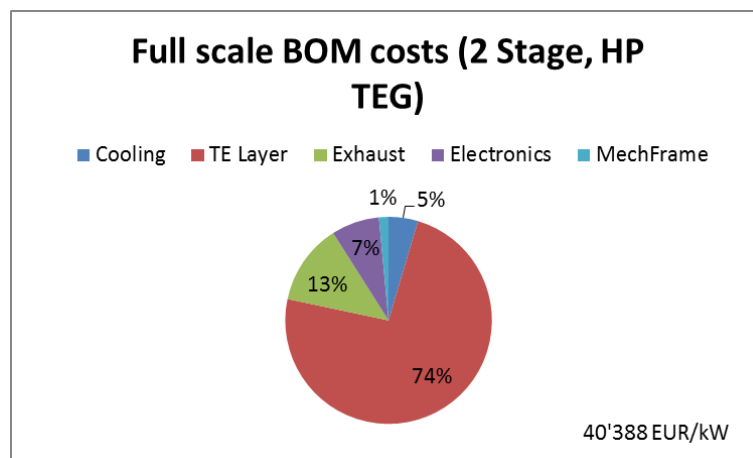


Figure 37: BOM cost split of full scale TEG with high performance modules (prototype)

Figure 37 shows the relation based on a high performance HP module (see chapter 3.2.2.3) prototype cost and considers an upscale in production while using the current manual manufacturing process of heat collector tubes and coolers in order to build one full scale prototype. The electronic concept as described in chapter 3.2.3 is maintained, thus leading to a moderate increase in production volumes with cost reduction effects. The cost split is based to 98 % on supplier quotes. The EUR/W relation is about 13-14 times higher than the expected market feasibility.



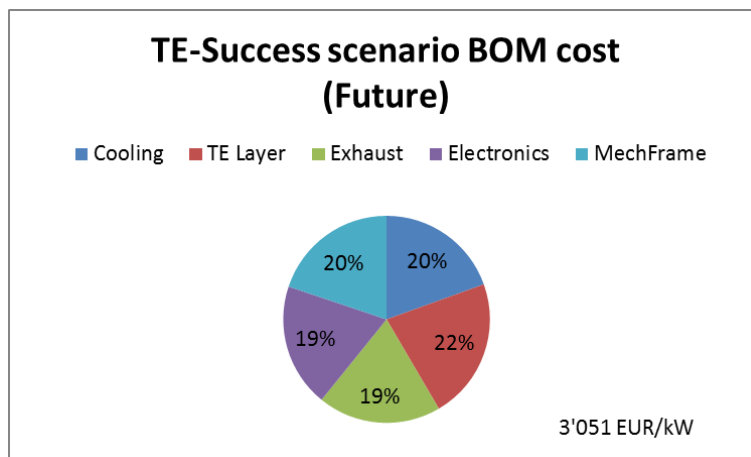


Figure 38: BOM cost split of full scale TEG with high performance modules in case of market penetration

Figure 38 shows the relation based on the assumption that the HP modules penetrate the market at a cost of ≤ 5 EUR per module (high volume scenario) [22]. Heat collector tube and coolers are manufactured at 20-25 EUR/component in a highly optimized, large scale processes (e.g. using conveyor oven brazing or vacuum oven brazing). To reach this cost level the production volumes of the single components have to significantly increase, therefore the TEG has to address the full CHP segment (e.g. from Nano-CHP to Large-CHP).

The **manufacturing costs** of the TEG system can be assessed after reviewing and optimizing the manufacturing process as it was described in chapter 3.3. The current prototype process is not representative for the final serial process as its assembly invoked stages of trial and error. In the future, continuous improvement and design simplification (e.g. of the wiring harness) will lead to a significant cost reduction. It is assumed that the manufacturing process will add up to 40 - 50 % to the overall TEG costs.

Operation and maintenance costs for the TEG can be expected to be very low. Due to exhaust gas exposure, the TEG should require the same maintenance as a standard heat exchanger, thus the cleaning interval should be scheduled every 10 000 hrs or 1.5 - 2 years and will last for about 7 - 8 hrs. Costs are in the range of 1 300 - 1 800 EUR per service [23]. The long term stability of the thermoelectric converters is still under investigation. They are considered to be maintenance free within the typical CHP usage period of 10 years (The degradation they will show after such a period is not clear today).

Recycling of TE-material like Bi_2Te_3 is still under ongoing development and costs cannot be estimated. Due to EU directives like 2002/95/EG (ROHS-1) and 2002/96/EG (ROHS-2) recycling of electronics has become part of national legislation and needs to be addressed in the future.

Projected TEG system price

In the following chapters the target price of a TEG in serial production is assumed to be 44 000 EUR at an electricity production of 11 kW_{el} (4 000 EUR/kW). This target price is derived from the market situation as well as from the cost expectations as explained



above. The maintenance schedule is in line with a classical heat exchanger and takes place every 10 000 hrs at a cost of 1 800 EUR. Full installation cost in Braunschweig is 4x 44 000 EUR or 176 kEUR resulting into an installed capacity of maximum 44 kW_{el}.



4. Comparative analysis of H2P systems

This chapter gives a techno-economical comparison of the two systems HT-SCR and TEG.

4.1. System performance impact

To assess the technical impact of various H2P systems on the CHP performance it is necessary to analyse the full energy flow inside the CHP. A simple, but powerful way to visualize the result is a Sankey diagram.

Performance of CHP with HX

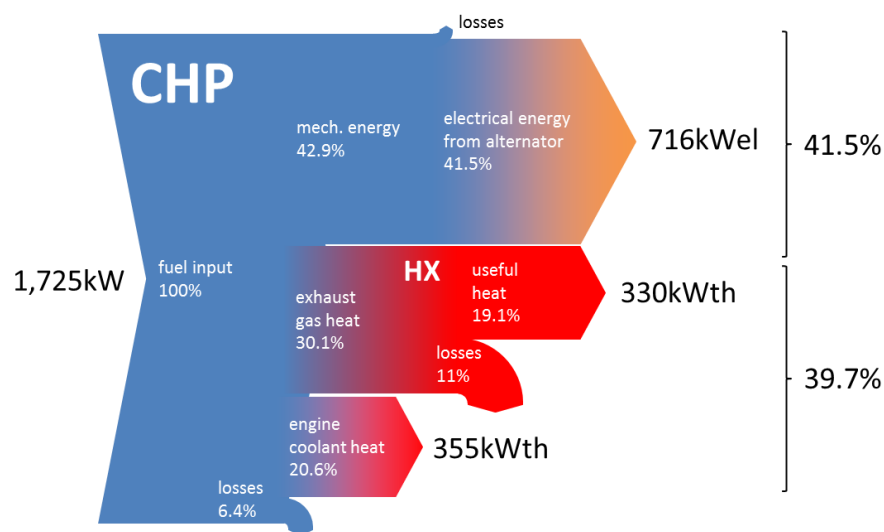


Figure 39: Energy flow diagram of the MWM 50Hz PT 20128 KA in Braunschweig (based on datasheet [14])

Figure 39 shows the energy flow diagram of a single CHP unit in Braunschweig that is equipped with an exhaust gas heat exchanger (HX). It is based on the manufacturer's data sheet provided in [14]. In the diagram 1,725 kW of chemical energy in the form of biogas are converted into 41.5 % (716 kW_{el}) electrical energy and 39.7 % (685 kW_{th}) heat that can be extracted both from the engine cooling circuit (305 kW_{th}) and the engine exhaust (330 kW_{th}). Approximately 11 % are lost in the chimney of the plant, as the final exhaust temperature is 180 °C.

Performance of CHP with HT-SRC

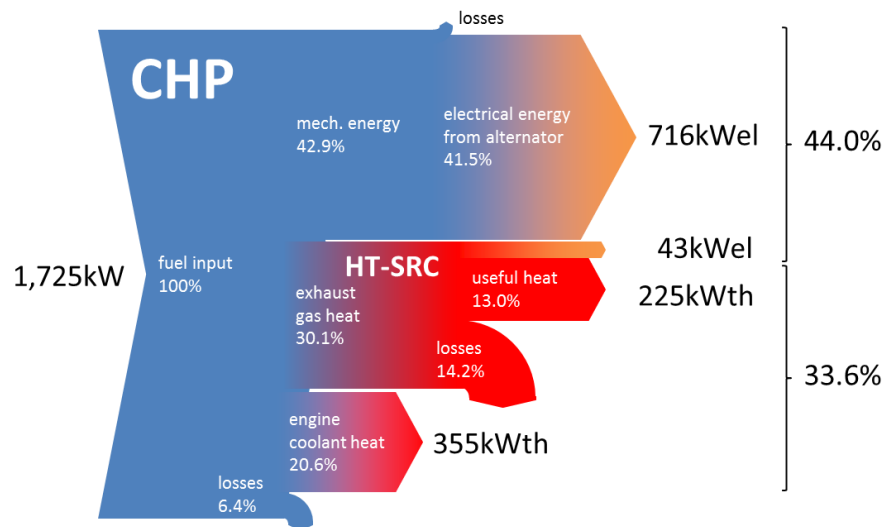


Figure 40: Energy flow diagram of the MWM CHP with HT-SRC (according to preliminary manufacturer datasheet, without additional heat collect system)

The manufacturer CONPOWER Technik Projekt GmbH & Co. KG expects the HT-SRC to reach an electrical efficiency of approximately 15%, converting 282 kW_{th} of exhaust heat into 43 kW_{el} of electrical power [24]. 225 kW_{th} are injected into the cooling system (without additional heat recovery) [24]. Without the additional heat recovery system the unit utilises approx. 54% of the available heat in the exhaust gas. The electrical efficiency is raised from 41.5% to 44% (+6%). Thermal efficiency is reduced to 33.6%. It should be acknowledged that this analysis is based on preliminary data and the self-consumption of the unit is not considered. It is assessed with 6 - 8% of the electrical output of the HT-SRC unit [24].

Performance of CHP with TEG

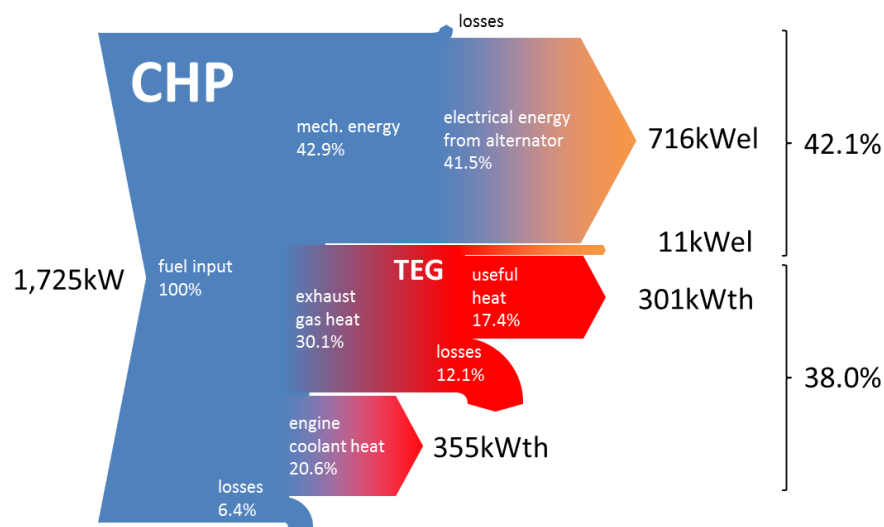


Figure 41: Energy flow diagram of CHP with TEG (full-scale, two-stage TEG, based on bench test, without additional heat collect system)



Figure 41 shows the performance of the CHP with a full-scale TEG system as it was described in chapter 3.5. Based on the same power input as the other two scenarios, the electrical performance of the CHP is raised by about 11 kW_{el} reaching 42.1 % (+1.5 %). As there is also no additional heat collect system, the thermal performance is slightly degraded to 38 %. Chimney heat losses are about 12.1 %. Electrical conversion losses in the power electronics and possible auxiliary power consumption are not considered. They are expected to be approx. 5-10 % of the electrical output of the TEG.

Table 12: Summary of impact of heat-2-power system on the overall performance of the CHP.

	Gross Electrical Efficiency (rel.)	Thermal Efficiency (rel.)	Overall Efficiency (rel.)
CHP HX (Reference)	41.5% (± 0%)	39.7% (± 0%)	81.2% (± 0%)
CHP HT-SRC	44.0% (+ 6%)	33.6% (- 15.3%)	77.6% (- 4.4%)
CHP TEG	42.1% (+ 1.5%)	38.0% (- 14.0%)	80.1% (- 1.4%)

From the direct comparison in Table 12 it can be concluded that both studied H2P systems degrade the thermal efficiency of the CHP. Case by case this can be compensated by installing an additional heat recovery system (heat collect system). Regarding the possible electrical efficiency increment for CHP units in the size of the installation in Braunschweig, the prospected benefit gained with the SRC unit outperforms the TEG by at least factor of 4.

Moreover literature indicates that the benefit of SRC/ORC could be even higher. In [25] an HT-ORC system was combined with a similar gas engine as it is installed in Braunschweig. As a result, an increase of the total electrical power output of about 8 % could be realized (based on rated power of engine of 716 kW_{el}). In field deployment the high temperature ORC-unit developed by Fraunhofer Umsicht and Dürr Cyplan reached a gross electrical efficiency (without considering auxiliary power needed to run the system) of about 17 to 21 %, depending on the input heat flow rate. It is expected that by using an ORC-unit in combination with modern high performance CHP engines that can have electrical efficiencies of 44 to 46 % the total electrical efficiency can be increased to up to 47 to 49 % [25].

In the next chapter, the performance benefit will be put in relation with the system costs.

4.2. Economic impact analysis

4.2.1. Direct comparison

The economic impact analysis of the H2P systems is based on a return on investment ROI, simple payback period PP and net present value NPV calculations. For the direct comparison, the data of an HT-ORC system installed in AZV Südholstein, Hetlingen [26] and a full scale TEG prognosis for all four CHP units in Braunschweig are analysed (see chapters 3.5 and 3.6). One main difficulty observed when comparing the two systems is



the difference in size (heat intake) and utilisation rate. In addition, heat production and valorisation is neglected, as there is no data available for the ORC unit.

The following electricity price data is assumed as evaluation basis for the analysis.

Table 13: Electricity price components [27].

Price component	EUR/MWh
Electricity energy price	52.60
Grid fee	30.20
EEG fee	63.54
Electricity tax	15.77
Concession fee	1.10
Miscellaneous fees	8.63
VAT	32.65
Sum	204.49

The electricity value used is valid for self-consumption of electricity inside the WWT plant. If electricity is sold on the market, the value will be market price plus premium. Studies have discovered that it is more economic to use produced electricity to cover internal demand [27].

The following equation is used to calculate return of invest ROI over the utilization period [28, 29]:

$$\text{Equation 18 } ROI = \frac{(\text{Gain of Investment} - \text{Cost of Investment})}{\text{Cost of Investment}}$$

The time frame for the ROI observation is the typical utilization period of 10 years [26]. During this time the benefit of producing self-consumed electricity on-site and the cost of investment (including maintenance and operation) of the H2P units are compared.

To simplify the comparison, it is assumed that only equity and no borrowed capital is used for the investment. Furthermore it is taken as basis that the total sum of the investment is paid at the beginning of the utilization period. The interest rate on the invested capital is neglected. The annual gain of investment is calculated from the annual electricity yield minus the annual maintenance cost. The gain of investment is calculated by multiplying the annual gain with the typical utilisation period.

The simple payback period PP of the TEG unit can be calculated as follows, when the annual recovery is constant [29, 30]. Also here, the interested rate on capital is neglected for simplicity reasons.

$$\text{Equation 19 } PP = \frac{\text{Initial Investment}}{\text{Annual Recovery}}$$



The result indicates the number of years a system has to be minimum operated in order to have a positive cost benefit ratio.

In addition to the ROI and the PP the net present value (NPV) of the two investments was calculated to further assess their benefit. The calculation is based on the net present value method, in which all future earnings Er and expenditures Ex including initial invest, operating and maintenance costs during the utilization period t of the unit are discounted (with a certain interest rate r) to determine their current value [29, 31].

$$\text{Equation 20 } NPV_{\text{Invest}} = \sum_{t=0}^n (Er_t - Ex_t) \cdot (1 + i)^{-t}$$

Balancing all present values, results in the NPV of the investment. In case the NPV is > 0 the investment would add value that is higher than just the interest rate⁶. A NPV < 0 is unfavourable for an investor since the expected interest rate is not reached.

For the following two cases it was assumed that the TEG-, and ORC-units have a terminal value of 0 EUR after 10 years and that only equity was used. The purchasing and installation costs were assumed to be part of an initial invest at the beginning of the utilization period ($t=0$). Furthermore no additional risk loading was applied. For the interest rate a value of 5 % was chosen based on literature⁷.

Braunschweig: 4 CHP units with 4 TEGs

The four TEG systems in Braunschweig are considered to be operated on a nominal exhaust heat input of 312 kW_{th} each, producing nominal 11 kW_{el} electrical power and 201 kW_{th} of useful heat each (see chapter 3.5). The expected gross electrical efficiency of the TEG is 3.5 %. The annual utilization is 4 207 hrs per gas engine⁸ or 16 828 hrs in total for all 4 gas engines. The contribution of the TEGs to the overall annual electricity production would reach around 1.5 %.

⁶ Example: NPV=50.000 EUR → The investor receives the invested capital, an interest payment of 5 % and additionally about 50.000 EUR [29].

⁷ Pili et al. used 4 % [32] as a discount rate to compare different ORC-configurations used for waste heat recovery applications, in a study by the Fraunhofer ISE [31] values of about 2.4 to 7.7% were specified as real weighted average cost of capital for different renewable and non-renewable power plants, the VGB PowerTech e.V. used values of 4 to 7 % to compare the electricity costs of different renewable and non-renewable power plants [37].

⁸Information provided by NEAS A/S. CHP operating hours have been simulated and optimized in [26]. In average in Braunschweig, there are typical 2 out of 4 units in operation. The utilization rate per single CHP unit is around 48%.



Table 14: ROI and simple payback period calculation of TEG in Braunschweig.

Purchasing and installation costs	176 000	EUR
Specific investment costs ⁹	4 000	EUR/kW _{el} (nominal)
Utilization period	10	Years
Annual operation costs	4 800 ¹⁰	EUR/a
Annual operation time	4 207	Hours
Electricity production	185 108	kWh/a
Electricity yield	37 853	EUR/a
Annual gain of investment	+ 33 053	EUR/a
ROI	69	%
Simple payback period	5.3	Years
NPV of investment¹¹	+ 79 224	EUR

ORC System in AZV Südholstein

The WWTP Hetlingen in Südholstein was built in 1973 and has a capacity of 860 000 PE or 31 billion cubic meters of waste water per year. The annual electricity consumption of the plant is approx. 23 000 MWh and around 70 % or 18 000 MWh are produced on site, using CHP technology with an attached organic rankine cycle [26].

⁹ Target value (see chapter 3.6)

¹⁰ Assuming maintenance of each TEG every 1.5 years at a cost of 1 800 EUR (see chapter 3.6)

¹¹ Based on an interest rate of 5 %, 10 years utilization, terminal value after 10 years is 0 EUR.



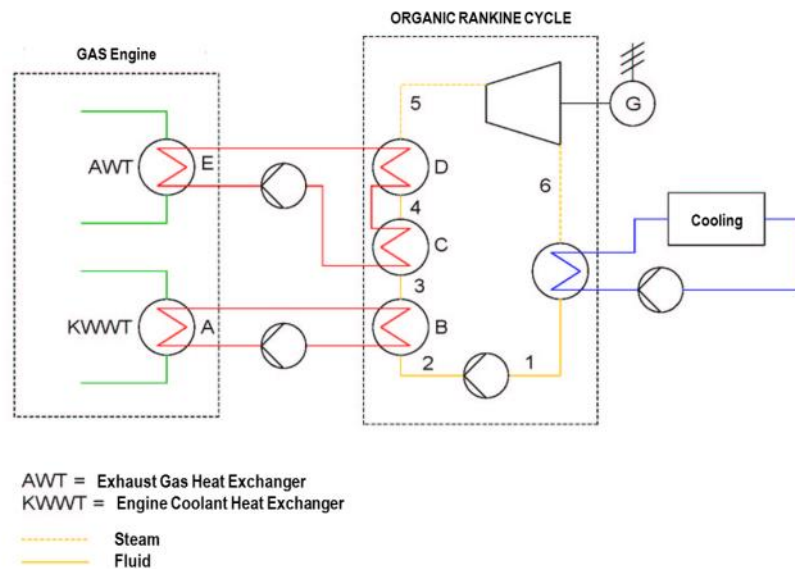


Figure 42: ORC implementation scheme in AZV Südholstein¹²

The ORC process used is very similar to the SRC explained in chapter 1.2.1. Instead of water the ORC unit of this plant uses a mixture of H₂O and iso-pentane as operating fluid. It is pumped towards a heat exchanger (B), where it is pre-heated by a secondary engine coolant circuit. In a second heat exchange stage (C) it is indirectly heated by exhaust gas heat and in a third stage (D) it is evaporated, producing superheated steam. Typically this secondary circuit is operated based on thermal oil circuit (E) [32]. The super-heated steam is expanded via a turbine that drives an electrical generator (G). In a condensing stage, the ORC fluid is again condensed.

According to the operator AZV Südholstein the ORC circuit operates on a nominal heat input of 1 072 kW¹³ and produces 144 kW_{el}¹⁴ power. The resulting gross electrical efficiency of the ORC is 13.4 %. The annual utilization is 2 500 hrs¹⁵. The contribution of the ORC to the overall annual electricity production is around 1.7 %.

¹² Original image was provided by azv Südholstein, Dr. Julia Weilbeer, division manager production; translation to English by Fraunhofer IPM

¹³ Data provided by azv Südholstein, Dr. Julia Weilbeer, division manager production

¹⁴ Data provided by azv Südholstein, Dr. Julia Weilbeer, division manager production

¹⁵ Data provided by azv Südholstein, Dr. Julia Weilbeer, division manager production

Table 15: ROI and simple payback period calculation of ORC in AZV Südholstein.

Purchasing and installation costs ¹⁶	475 000	EUR
Specific investment costs	3 299	EUR/kW _{el} (nominal)
Utilization period	10	Years
Annual operation costs	9 000	EUR/a
Annual operation time	2 500	Hours
Electricity production	360 000	kWh/a
Electricity yield	73 616	EUR/a
Annual gain of investment	+ 64 616	EUR/a
ROI	30	%
Simple payback period	7.4	Years
NPV of investment¹⁷	+ 23 951	EUR

In case the annual operation time of the ORC unit in AZV Südholstein would equal that of the TEG in Braunschweig (4 207 h instead of 2 500 h) the following values would be obtained, assuming the operation/maintenance costs scale linear with the operation time: ROI = 98 %, PP = 4.4 years, NPV = + 364 634 €. In that case the investment would be much more favourable compared to the TEG.

Discussion of result

From this result it can be concluded that the TEG installation in Braunschweig has a smaller annual gain and much lower investment costs when compared against the ORC installation in Hetlingen. It potentially amortizes quicker, in a period of about 5.3 years. The net present value of both systems is positive, making them both reasonable investments. Of course this result is based on several assumptions, which have been described in previous chapters. One important key for the TE technology is achieving a system price level of $\leq 4\,000$ EUR/kW_{el}. Today this is only likely to be reached in high volume production scenarios (automotive or consumer market) and not in the niche market of large scale CHP.

It should be noted that the two WWTP are different in their size (350 000 PE vs. 860 000 PE) and H2P system utilization rates (4 207 hrs vs. 2 500 hrs), as well as the fact

¹⁶ Data provided by azv Südholstein, Dr. Julia Weillbeer, division manager production

¹⁷ Based on an interest rate of 5 %, 10 years utilization, terminal value after 10 years is 0 EUR.



that the Braunschweig scenario uses 4 CHP and TEG units rather than just one ORC unit. The result may give a first indication that TEG is a technology that is favourable for smaller CHPs.

The heat production is not valorised in this study, however the heat in- and output of the two systems is considerably different. According to available data the TEG heat uptake is about 2 times higher (5 250 MWh_{th} (TEG) vs. 2 680 MWh_{th} (ORC)). Consequently, the useful heat generated by the two systems will significantly differ. Due to its direct integration, TE technology has a potentially higher capability of generating useful heat (=heat injected a heating/cooling circuit e.g. for remote heating applications).

4.2.2. Levelized cost analysis

To put the result of chapter 4.2.1 into a more global context, a Levelized Cost of Electricity (LCOE) is a common measure used to compare different technologies of electricity production based on the lifetime costs (investment cost, operation and maintenance costs and fuel costs). It is described in [33], [34], [35]. Over an assumed lifetime the sum of costs are divided by the sum of electrical energy produced. Additionally the LCOE takes into account the discount rate over the lifetime [35]:

$$\text{Equation 21 } LCOE = \frac{\sum_{k=1}^n \frac{C_k}{(1+i)^k} + C_0}{\sum_{k=1}^n \frac{E_k}{(1+i)^k}}$$

where i is the interest rate, n the assumed life time, C_k are the yearly maintenance costs, C_0 are the investment costs, E_k is the yearly electricity production. In all cases, the yearly maintenance costs. A period n of 10 years is considered, and the interest rate amounts $i = 5\%$ (see 4.2.1).

Pili et al. 2017 [35] simulated the performance of different ORC-units to recover electricity from fluctuating heat sources. Depending on the heat source (clinker cooling, flue gas from an electronic arc furnace or a reheating furnace) and the additional usage of sensible or latent heat storage facilities, they calculated that a LCOE as low as 5.5 to 8.9 Eurocent/kWh could be reached (discount rate = 4 %, annual operation = 7 000 - 8 000 hrs/a) [35]. According to a study by Ueckerdt et al. in comparison, the System-LCOE for renewable energy technologies like wind and solar PV are about 7 to 10 Eurocent/kWh and 12 to 22 Eurocent/kWh respectively depending on the final electricity share of the technology [34]. The Fraunhofer ISE also investigated the LCOE for different renewable and non-renewable power generating technologies in 2013 [31]. Their findings are summarized in Figure 43.



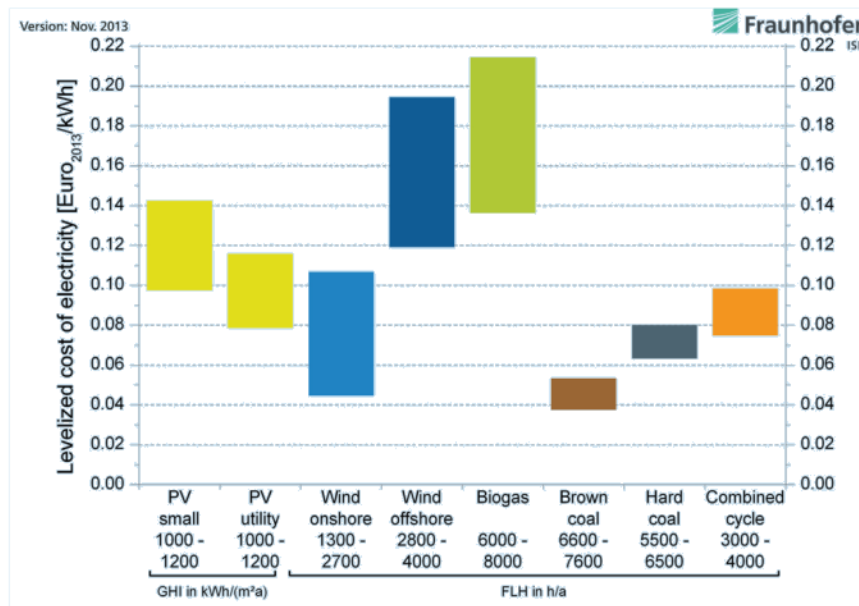


Figure 43: LCOE for various renewable energy sources [31]

Based on the specific use case values from Table 14 and Table 15 for the TEG or the ORC-unit the corresponding LCOE values can be calculated to be 15 Eurocent/kWh (TEG) and 20 Eurocent/kWh (ORC). Consequently the future TEG is based in a competitive cost range among electricity production from Biogas technology; however, as also explained above ORC could potentially be cheaper when higher annual operation times can be achieved.

4.3. Summary

Based on the Braunschweig scenario, the TE-technology allows raising the CHP electrical yield by +1.5%. Assuming a future specific investment cost of 4 000 EUR/kW_{el}, it is expected to amortize in minimum 5.3 years. Its potential main benefits are the low investment costs as well as the low operation and maintenance cost. Due to its direct integration, the thermal performance of the TEG is likely to be better in comparison with SRC/ORC technology. The levelized cost of electricity production from the TEG is around 15 ct/kWh assuming an annual operational utilization of 4 207 h/a.

For the studied CHP size of 710 kW_{el}, SRC outperforms TEG by a factor of 4-5 in electricity production. The electrical yield improvement could reach up to +6% for SRC or even +8% in case of usage of ORC [25]. Despite the fact that both investment costs and maintenance costs are higher than for TEG, new ORC technology could allow reaching a levelized cost of 5.5 to 8.9 ct/kWh [35]. However, existing ORC implementations like in WWTP Hetlingen can also range at lower values with 20 ct/kWh (2 500 h/a). The amortization of ORC can be achieved in less than 5 years, if sufficient operation times are reached.



5. Summary and Conclusion

The EU-funded project "POWERSTEP" aims on a full scale demonstration of energy positive sewage treatment plant concepts towards market penetration. In different case studies, innovative technologies for waste water treatment plants (WWTP) are developed, deployed and assessed.

This report introduces different heat-to-power technologies; it described in detail the design and manufacturing and field deployment of a TEG for the CHP installation in Braunschweig and it concludes with a comparative technico-economical analysis of the two technologies of thermoelectric conversion and Rankine cycle (ORC/SRC).

The construction and design of the thermoelectric generator has been closely aligned with the CHP system of the case study site in Braunschweig. One of the main important topics was the selection of the right thermoelectric material for the application temperature range: High performance Bi₂Te₃ was chosen to be the best solution for exhaust gas temperatures of 450°C-180°C and coolant temperatures of 60-80°C. For the pilot integration, several possible positions on the exhaust line have been studied and measurement electronics along with a safety concept have been developed and deployed. The final implementation and field tests lead to important insights on practical issues, like the operation in harsh industrial environment and more. The lessons learned give an important input for the future development of TEG.

The comparative technico-economical analysis based on the Braunschweig scenario showed, that the TE-technology allows raising the CHP electrical yield by +1.5 %. Assuming a future specific investment cost of 4 000 EUR/kW_{el}, it is expected to amortize in approximately 5.3 years. As today some prototype part costs are still more than 10 times higher than targeted, the authors expect that a significant impact is needed from high volume markets in order to reach into the target cost ranges for this application class. The supply chain for the technology is still under development and the main building blocks are heat exchangers, thermoelectric modules and power electronics.

In direct comparison with SRC/ORC technology, potential main benefits of thermoelectrics are low investment costs as well as the low operation and maintenance cost. The levelized cost of electricity production from the TEG could be around 15 ct/kWh (with a utilization of 4 207 h/a).

For the studied CHP size of 710 kW_{el}, using SRC potentially outperforms the TEG by a factor of 4-5 in electricity production. The electrical yield improvement could reach up to +6 % for SRC or even +8 % in case of usage of an ORC. Despite the fact, that both investment costs and maintenance costs are higher than for TEG, new ORC technology could allow reaching a levelized cost of electricity of 5.5 to 8.9 ct/kWh. However, existing ORC implementations like in WWTP Hetlingen can also range at higher values with 20 ct/kWh (with a utilization of 2 500 h/a).

It can be concluded that a future TEG would be based in a competitive cost range among electricity production from Biogas technology; however, as explained above the latest ORC technology could be potentially cheaper and more effective in this application class. The results may give a first indication that TEG is a technology that is favourable for smaller CHPs.



6. Bibliography

- [1] ARCTIK S.P.R.L., "Powerstep Project Homepage," 2017. [Online]. Available: <http://www.powerstep.eu/>. [Accessed 13 12 2017].
- [2] UK Government - Department of Energy and Climate Change DECC, "CHP Technology - A detailed guide for CHP developers - Part 2," Crown, London, 2008.
- [3] US Department of Energy, "Combined Heat and Power Technology Fact Sheet Series," DOE, 2017.
- [4] L. W. X. W. G. J. Xiaojun Zhang, "Comparative study of waste heat steam SRC, ORC and S-ORC power," *Applied Thermal Engineering*, pp. 1427-1439, 17 June 2016.
- [5] T. J. S. a. L. A. D. George R. Schmidt, "Radioisotope Power: A Key Technology for Deep Space Exploration," in *Radioisotopes - Applications in Physical Sciences*, USA, INTECH (www.intechopen.com), 2011.
- [6] K. R. Tarantik, J. D. König, M. Jäggle, J. Heuer, J. Horzella, A. Mahlke, M. Vergez and K. Bartholomé, "Thermoelectric Modules Based on Silicides – Development and Characterization," *Materials Today: Proceedings, Vol.2(2)*, pp. 588-595, 2015.
- [7] R. Kühn, O. Koeppen, P. Schulze and D. Jänsch, "Comparison between a Plate and a Tube Bundle Geometry of a Simulated Thermoelectric Generator in the Exhaust Gas System of a Vehicle," *Materials Today: Proceedings, Vol.2(2)*, pp. 761-769, 2015.
- [8] "EU-FP7 NMP Project 263207 Thermomag," CORDIS Forschungs und Entwicklungsinformationsdienst der Gemeinschaft, 26 05 2017. [Online]. Available: http://cordis.europa.eu/project/rcn/98971_de.html. [Accessed 26 01 2018].
- [9] K. Bartholomé, B. Balke, D. Zuckermann, M. Köhne, M. Müller, K. Tarantik and J. König, "Thermoelectric Modules Based on Half-Heusler Materials Produced in Large Quantities.," *Journal of Electronic Materials* 43 (2013), Nr. 6, pp. 1775-1781, 2013.
- [10] M. D. M. K. K. R. T. Martin Rosenberger, "Vehicle Integration of a Thermoelectric Generator," *MTZ worldwide, Volume 77, Issue 4*, pp. 36-43, 2016.
- [11] SE|BS, "Stadtentwaesserung-Braunschweig," Stadtentwaesserung-Braunschweig, 2017. [Online]. Available: <http://www.stadtentwaesserung-braunschweig.de/>. [Accessed 13 12 2017].
- [12] Top Agrar, "Aus Abwärme wird Strom," *Energiemagazin 2015*, pp. 8-11, Januar 2015.
- [13] H. C. Christian Bücherl, "BHKW-Ratgeber.de," [Online]. Available: <http://www.bhkw-ratgeber.de/>. [Accessed 09 02 2018].
- [14] MWM Caterpillar Energy Solutions GmbH, *Technische Daten 50 Hz PT 1028 KA Braunschweig*, Mannheim , 2008.



- [15] DEKRA Automobil GmbH, "Bericht 553161977 Klärwerk Steinhof," DEKRA Automobil GmbH, Braunschweig, 2015.
- [16] Badenova AG, "Badenova Innovationsfonds," Badenova AG, 2015. [Online]. Available: <https://www.badenova.de/web/%C3%9Cberuns/Innovationsfonds/index.jsp>. [Accessed 14 12 2017].
- [17] Fraunhofer Institut für Physikalische Messtechnik, "Abwärmeverstromung - Projekt TE-BHKW," Fraunhofer Institut für Physikalische Messtechnik, 2016. [Online]. Available: <https://www.ipm.fraunhofer.de/de/gf/energiewandler-thermische/anw/abwaerme-nutzung-verstromung/projekt-te-bhkw.html>. [Accessed 09 2 2018].
- [18] VDI-Gesellschaft Verfahrenstechnik und Chemieingenieurwesen, VDI Heat Atlas, Second Edition, Heidelberg: Springer Verlag, 2010.
- [19] M. Freunek, Untersuchung der Thermoelektrik zur Energieversorgung autarker Systeme, Freiburg im Breisgau: Der Andere Verlag, 2010.
- [20] A. Montecucco, Efficiently maximising power generation from thermoelectric generators, Glasgow: University of Glasgow, 2014.
- [21] J. H. H. Carstens, Control and Optimization of a DC-DC Converter for Thermoelectric Generators, Berlin: Universität Berlin, 2016.
- [22] K. Bartholomé, J. Heuer, J. Horzella, M. Jäggle, J. König and K. Tarantik, "Thermoelectric modules built with new high-temperature materials," in *IAV - 4th Thermoelectrics Conference, Berlin, Germany*, Berlin, 2014.
- [23] Top Agrar, "Freie Fahrt für warme Luft," *Energiemagazin 2013*, pp. 28-31, April 2013.
- [24] CONPOWER Technik GmbH & Co. KG, "Datenblatt HT SRC Feldtestanlage R4S Stand 17.06.2013," CONPOWER Technik GmbH & Co. KG, Kaufungen, 2013.
- [25] Fraunhofer-Institut für Umwelt-, Sicherheits- und Energietechnik UMSICHT, "Abschlussbericht Entwicklungs-/Demonstrationsprojekt mit Feldversuch "ORC-Prozesse zur Abwärmenutzung an BHKW-Motoren" Feldversuch ORC FKZ-Nr. 0327436C," Fraunhofer UMSICHT, Oberhausen, 2013.
- [26] A. Südholstein, "Abwasser Zweckverband Südholstein," AZV Südholstein AÖR, [Online]. Available: <https://www.azv.sh/>. [Accessed 07 02 2018].
- [27] L. H. Ravn, "POWERSTEP: Recommendations for improved energy management at waste water treatment plants," Neas Energy A/S, 2017.
- [28] Investopedia, "Return On Investment - ROI," [Online]. Available: <https://www.investopedia.com/terms/r/returnoninvestment.asp>. [Accessed 23 02 2018].
- [29] A. Daum, W. Greife and R. Przywara, *BWL für Ingenieure und Ingenieurinnen - Was man über Betriebswirtschaft wissen sollte*, Wiesbaden: Vieweg+Teubner Verlag /



GWV Fachverlage GmbH Wiesbaden, 2010.

- [30] Investopedia, "Payback Period," [Online]. Available: <https://www.investopedia.com/exam-guide/cfa-level-1/corporate-finance/payback-period.asp>. [Accessed 23 02 2018].
- [31] FRAUNHOFER-INSTITUT FÜR SOLARE ENERGIESYSTEME ISE, "STROMGESTEHUNGSKOSTEN ERNEUERBARE ENERGIEN," Fraunhofer ISE, Freiburg, 2013.
- [32] U. Drescher and D. Brüggemann, "Fluid selection for the Organic Rankine Cycle (ORC) in biomass power and heat plants," *Applied Thermal Engineering* 27 (1), p. 2006, 24 04 223–228.
- [33] US Department of Energy, "US Department of Energy - Levelized Cost of Energy (LCOE)," 08 2015. [Online]. Available: <https://energy.gov/sites/prod/files/2015/08/f25/LCOE.pdf>. [Accessed 12 02 2018].
- [34] F. Ueckerdt, L. Hirth, G. Luderer and O. Edenhofer, "System LCOE. What are the costs of variable renewables?," *Energy* 63; DOI: 10.1016/j.energy.2013.10.072, p. 61–75, 10 2013.
- [35] R. Pili, A. Romagnoli, H. Spliethoff and C. Wieland, "Techno-Economic Analysis of Waste Heat Recovery with ORC from Fluctuating Industrial Sources," *Energy Procedia* 129 (Supplement C); DOI: 10.1016/j.egypro.2017.09.170, p. 503–510, 09 2017.
- [36] US Department of Energy, "Combined Heat and Power Technology Fact Sheet Series," DOE, 2017.
- [37] VGB PowerTech e.V., Levelised Cost of Electricity LCOE 2015, Essen: VGB PowerTech Service GmbH, Verlag technisch-wissenschaftlicher Schriften, 2015.



